

# TITLE. Target confinement in small reaction volumes using microfluidic technologies: A smart approach for single-entity detection and analysis

AUTHOR NAMES. Karen Ven<sup>+a</sup>, Bram Vanspauwen<sup>+a</sup>, Elena Pérez Ruiz<sup>a</sup>, Karen Leirs<sup>a</sup>, Deborah Decrop<sup>a</sup>, Hans Gerstmans<sup>a,b,c</sup>, Dragana Spasic<sup>±a</sup>, Jeroen Lammertyn<sup>±\*a</sup>

AUTHOR ADDRESS. <sup>a</sup>Department of Biosystems, KU Leuven - University of Leuven, Willem de Croylaan 42, 3001 Leuven, Belgium. <sup>b</sup>Department of Applied biosciences, Ghent University, Valentyn Vaerwyckweg 1 - building C, 9000 Gent, Belgium. <sup>c</sup>Department of Biosystems, KU Leuven - University of Leuven, Kasteelpark Arenberg 21, 3001 Leuven, Belgium

<sup>+</sup>Contributed equally to this work. <sup>±</sup>Contributed equally to this work. <sup>\*</sup>Corresponding author: jeroen.lammertyn@kuleuven.be

KEYWORDS. *Microfluidics, single molecule detection, single-cell analysis, cell, nucleic acid, protein, confinement, bio-sensor*

---

**ABSTRACT:** Over the last decades, the study of cells, nucleic acid molecules and proteins has evolved from ensemble measurements to so-called single-entity studies. The latter offers huge benefits, not only as biological research tools to examine heterogeneities among individual entities within a population, but also as biosensing tools for medical diagnostics, which can reach the ultimate sensitivity by detecting single targets. Whereas various techniques for single-entity detection have been reported, this review focusses on microfluidic systems that physically confine single targets in small reaction volumes. We categorize these techniques as droplet-, microchamber- and nanostructure-based and provide an overview of their implementation for studying single cells, nucleic acids and proteins. We furthermore reflect on the advantages and limitations of these techniques and highlight future opportunities in the field.

---

In recent years, the approach of studying cells, nucleic acid (NA) molecules and proteins, collectively defined here as ‘entities’, is experiencing a transition from traditional methods, which provide the averaged response of an ensemble of molecules or cells, to single-entity studies. The latter offers major benefits, not only for the fundamental fields of molecular and cell biology, but also for more applied disciplines such as biosensing for diagnostics. From a biological point of view, these studies allow to examine individual entities within complex biological systems. This way, they provide more information on anomalous or exceptional species, which would be otherwise lost within the noise<sup>1,2</sup>. Thanks to that, the cell heterogeneity concept has been established, which considers heterogeneous characteristics as an intrinsic property of individual cells, grown in an identical environment<sup>3,4</sup>. Single-entity studies have also revealed other molecular diversities, such as the presence of rare mutations in a DNA sample<sup>5</sup>, differences in catalytic activities of individual enzymes<sup>6,7</sup> and unique kinetic processes of bioreceptor-protein interactions<sup>8,9</sup>. From a diagnostic perspective, the trend of targeting individual entities is of interest as well<sup>10</sup>. Whereas conventional detection methods are typically limited to measuring concentrations in the low picomolar (pM) range<sup>11</sup>, prominent disease biomarkers are often present at these concentrations only in a late stage of the disease. Hence, measuring concentrations in the low femtomolar (fM) or even attomolar (aM) range can provide valuable information for

**Microfluidic system:** Network of micrometer-sized channels in which fluids can be manipulated in a controlled way. **Microchamber:** Micrometer-sized space with solid side and bottom walls in which a single entity can be physically confined. **Dynamic range:** The range of target concentrations for which the sensor readout is proportional to the amount of target molecules in the sample. **High concentration limit:** limitation of single-entity techniques for quantifying high target concentrations due to the presence of more than one single entity per detection volume resulting in an underestimation of the true concentration. **Low concentration limit:** limitation of single-entity techniques for quantifying low target concentrations due to the large number of empty detection volumes, resulting in an increased analysis time.

early disease diagnostics. In order to reach these concentrations or study single-entity heterogeneities, approaches based on single-entity detection are increasingly investigated in recent times.

One of the first approaches for studying and detecting single entities was based on examining small parts of the complete sample in a serial fashion<sup>10</sup>. Here, detection was performed either by laser-scanning the sample with high resolution (e.g. confocal microscopy<sup>12,13</sup>) or by flowing the solution through a tightly focused laser spot, which detects

passing molecules or cells (e.g. flow cytometry<sup>14</sup>). Alternatively, individual entities can be captured on a surface and subsequently detected and studied (1) through a fluorescent label (e.g. total internal fluorescence<sup>15</sup>), (2) by applying a force in the piconewton regime (e.g. magnetic tweezers<sup>9</sup>, optical tweezers<sup>16,17</sup>) or (3) in a label-free manner by means of a scanning probe (e.g. atomic force microscopy<sup>18</sup>) or optical microcavities (e.g. whispering-gallery microcavities<sup>19</sup>).

The abovementioned approaches commonly interrogate only femtoliter (fL) volumes at once, implying that analysis of a sample containing few microliters ( $\mu\text{L}$ ) is very time-consuming. In addition, at low concentrations, over a million of these fL volumes have to be imaged before detecting a single target which, moreover, diffuses very slowly into the small detection volume<sup>20,21</sup>. Although this low concentration limit could be overcome by increasing the sample concentration, this poses new challenges for true single-entity detection as it increases the chance of encountering more than 1 entity in the observed volume. This is known as the high concentration limit and, together with the low concentration limit, poses a serious constraint on single-entity techniques. They are particularly restrictive in the field of biosensing, as samples with both low and high molecule concentrations are targeted, thus requiring a large dynamic range<sup>22</sup>.

Whereas some excellent reviews have been previously written, describing various single-entity detection methods<sup>10,23,24</sup>, here we will focus on those **approaches that rely on physical confinement of the individual entities in small containers, such as tiny droplets, microchambers or nanostructures**. These methods offer a smart strategy to overcome the previously described concentration limit. As it will be further illustrated, physically restricting the volume, accessible to a single entity, not only generates a high local concentration that is easier to detect<sup>25</sup>, but also allows for high-throughput and parallelized detection, pre-concentration of the target prior to confinement and signal amplification in the confined volume<sup>22,25</sup>. To confine single entities in small containers, the sample is commonly diluted in such a way that the quantity of single entities is much lower than the number of containers. Under this condition and according to Poisson statistics, the vast majority of containers does not contain any entity whereas the others contain only one<sup>26</sup>. Subsequent detection of the isolated entities generates either a negative (0 molecule) or a positive (1 molecule) signal in the confined volume, which represents the basis of a ‘digital’ readout. The total number of positive reactions in this digital assay can then be used for the quantification of the target in the original sample<sup>5</sup> and the properties of the isolated single entities can be analysed. For a more detailed explanation on the statistics behind single-entity studies, the interested reader is referred to the excellent reviews from Basu<sup>27,28</sup>.

Transportation and confinement of single entities into these small containers has been facilitated through microfluidic techniques<sup>23,29</sup>. This is largely related to the intrinsic advantages of microfluidics, including the capability of

handling small volumes with high precision, high throughput and in an automated and fast manner as well as the possibility to upscale fabrication at a reduced cost<sup>30,31</sup>. In general, microfluidic devices can be classified into: (1) continuous flow devices, i.e. those manipulating non-segmented flows in microchannels by using pumps and valves<sup>32</sup> or centrifugal forces<sup>33</sup> and (2) droplet-based devices, i.e. those manipulating individual fluid droplets<sup>34</sup> that are either immersed in an immiscible continuous phase within enclosed microchannels<sup>34</sup> (referred to as continuous-phase microfluidics (CMF)) or independently handled on a hydrophobic surface by means of electrostatic forces<sup>35,36</sup> (the latter known as digital microfluidics (DMF)). Both types of microfluidics have been used for isolating and studying individual entities and will be therefore addressed in this review.

In summary, this review provides an overview of the state-of-the-art microfluidic techniques for detection and analysis of physically confined single entities, being cells, NA molecules and proteins. For each type of entity, an overview is given of the reported confinement strategies (i.e. droplets, microchambers and nanostructures). Here, a special emphasis is on the following features: throughput, versatility, external components, fabrication procedure, dynamic range and multiplexing performance. In addition, Table 1 links the described confinement strategies with the application fields, provides a reference to selected papers and the commercially available devices. As such, the large body of literature is not only summarised from an entity-based but also a technology-based point-of-view. Lastly, the review is concluded with a summary and outlook of the future challenges and opportunities in the field.

## CELLS

---

Heterogeneous behaviour of cells under identical environmental conditions is a widely accepted concept. To study these heterogeneities, various single-cell analysis tools have emerged in the last years, many being based on microfluidic confinement of single cells in droplets or microchambers. In this review, single-cell studies will be categorized according to the target, which can be either (1) the complete cell, (2) the NA content or (3) the proteins, present in, secreted by or located on the surface of the single cell. It should be noted that these NAs and proteins, although originating from a single cell, are not analysed on a single molecule level. As such, the single-entity approach in these studies purely originates from the isolation of a single cell and not the subsequent analysis of the NAs and proteins of that cell, contrary to the other 2 sections in this review dealing with analysis of individually confined NA- and protein-entities.

### Single-cell detection

Detection of whole cells at the single cell level is important for a number of applications, such as growth evaluation<sup>37</sup>, viability studies<sup>38</sup> and drug screenings<sup>39</sup>. For this

purpose, single cells have been isolated within microfluidic systems in either droplets or microchambers (Table 1).

**Droplet-based** microfluidic systems have been used for the encapsulation and cultivation of a variety of single cells, including micro-algal cells<sup>37</sup>, bacteria<sup>40</sup>, yeast<sup>40,41</sup> and human cells<sup>42</sup>. In the latter study, for example, Clausell-Tormos *et al.* isolated both adherent and non-adherent single cells in individual picoliter- (pL) sized droplets for performing the growth assays. Although the droplets were generated through flow-focussing at a frequency of 800 droplets/second, the detection setup enabled analysis of only 500 droplets/second. The latter defines the true throughput of the system, but is not always specified in literature, which explains why the information in this review is often limited to the encapsulation rate.

In addition to this, more complex droplet-based microfluidic systems can be used for the screening of drugs at the single cell level, as demonstrated by Brouzes *et al.*<sup>39</sup> (Figure 1). Here, the drug library was first confined into aqueous droplets of 1 pL to 10 nanoliters (nL) using high-throughput flow-focusing (100 droplets/second), with each member of the library carrying a unique optical label. Subsequently, each library droplet was merged with a droplet containing a single human monocytic U937 cell, followed by collection and reinjection in a microfluidic chip in order to merge them with a second droplet, containing live/dead assay dyes. Finally, each droplet was analysed in terms of cytotoxicity and the drug-coding allowed to study the effect of the drugs in the library on the individual cells.

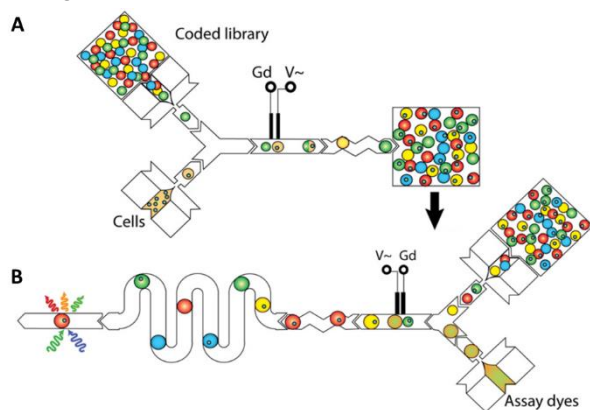


Figure 1. Droplet-based single-cell detection platform for drug library screening. A) The encoded drug library droplets were merged with a second droplet, containing a single cell. B) After off-chip incubation, the droplets were merged with a droplet, containing a live/dead dye and the effect of each library drug on the cells was evaluated. Adapted with permission from Ref.<sup>39</sup>.

It should be noted that the encapsulation of single cells is conventionally based on Poisson statistics<sup>31</sup>, as generating microdroplets from a highly diluted target solution results in less than 1 target per droplet on average. However, due to this dilution, the majority of droplets do not contain any target, resulting in the waste of reagents and the need to analyse a large number of droplets for low concentration

samples (defined in the introduction as the low concentration limit of single-entity techniques). This issue can be solved by applying a droplet sorting unit, discarding the empty droplets, which however decreases the overall throughput of the system<sup>43</sup>. As a more convenient solution, new methods have been established that provide passive self-alignment of the cells in an ordered stream, prior to their encapsulation in individual droplets<sup>44-46</sup>. By evenly spacing the cells in the stream through hydrodynamic interactions, the cell loading can be maximised in such a way that nearly every droplet contains a single cell, which aids in overcoming the low concentration limit while maintaining a high throughput.

In addition to droplet-based isolation, individual cells have been also confined in **microchamber**-based platforms to explore cellular heterogeneities<sup>47</sup>. One of the first applications hereof was demonstrated by the group of Walt<sup>48</sup>. They created ordered arrays of fL-sized wells by chemically etching the distal face of an optical fiber bundle to simultaneously study the viability and the pH dependency of individual adherent mouse fibroblast. Following this first application, numerous microwell array systems for single-cell studies have been reported in various materials (e.g. PDMS<sup>49-51</sup>, PEG-DA<sup>52,53</sup>, silicon wafers<sup>54</sup>) with diverse shapes and dimensions and with the number of wells ranging from hundreds<sup>49,55</sup> to thousands<sup>56,57</sup> and hundreds of thousands<sup>54</sup>. This increase in throughput of microfluidic platforms is an overall trend in the field (i.e. for both micro-chamber and droplet-based microfluidic systems), as the higher the number of chambers that can be confined and analysed in parallel, the higher is the chance to detect a single target in a sample with a low concentration. Importantly, microchamber-based systems offer the major advantage (over the droplet-based approaches) of docking single cells in the chambers, which simplifies long-term cell studies through their inherently fixed position, contrary to droplet-based systems where tracking of a single cell over a prolonged time is more complex. However, analysis of non-adherent cells in microchambers is less convenient as it generally requires the administration of cell-adhesives for an efficient cell isolation<sup>53,55</sup>, differing from droplet-based systems, which can be easily used for both adherent and non-adherent cell types.

However, the potential of microwell array platforms for the study of non-adherent stem cells is exemplified by Chin *et al.*<sup>58</sup>. They generated 10 000 microwells (20-500  $\mu\text{m}$  diameter, 10-500  $\mu\text{m}$  depth), which were treated with cell-adhesive proteins to increase the cell-occupancy. The array was integrated into a microfluidic culture chamber for improved automation and the injected cells were seeded through gravitational sedimentation. Using this platform, more than 3 000 single hippocampal progenitor cells were quantitatively tracked over 4 days and their differentiated progeny was imaged with conventional high magnification microscopy. Alternatively, the group of Folch reported a PDMS-based microwell array, reaching cell-seeding efficiencies above 85% for both adherent and non-adherent cells without the need for adhesive proteins, by optimizing microwell dimensions for gravitational sedimentation<sup>59</sup>.

This platform was integrated in a microfluidic system for the evaluation of odorant-evoked responses of ~2 900 single olfactory cells<sup>59</sup>. More recently, Kobayashi *et al.*<sup>38</sup> reported an approach for faster and more stable cell-seeding. Their PDMS-based platform contained 3 168 microwells (30  $\mu\text{m}$  diameter, 25  $\mu\text{m}$  depth), each with a pair of thin-film electrodes at the bottom (Figure 2) which enabled active seeding of single cells through dielectrophoretic (DEP) instead of gravitational forces. Moreover, the active trapping enabled fast reagent exchange while retaining the cells in the wells, without the need for complex valve systems. The platform was used for evaluating the viability of single cancer cells, but also for the evaluation of single-cell NAs and surface proteins (as addressed below in the corresponding sections), thereby providing a flexible tool for various single-cell studies.

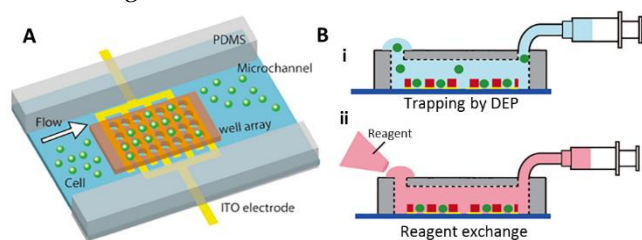


Figure 2. Microwell-based platform for single-cell viability studies. A) Schematic representation of the PDMS-based device containing a microfluidic channel with embedded microwells, fabricated on thin-film interdigitated electrodes. B) Schematic representation of (i) cell trapping through DEP forces and (ii) subsequent reagent exchange for viability studies. Adapted with permission from Ref.<sup>38</sup>.

Next to these continuous microfluidic flow systems with embedded microwells, an alternative approach was recently applied in our group for cytotoxicity studies on single non-adherent yeast cells (Figure 3)<sup>60</sup>. In this setup, 22 000 microwells (5.5  $\mu\text{m}$  diameter, 3  $\mu\text{m}$  depth) were etched in the grounding plate of a DMF platform and individual cells were trapped inside the wells by shuttling the sample droplet over the array through electrowetting-on-dielectric (EWOD). A fluorescence viability staining was used to evaluate the response of the individual cells to an antifungal drug in a spatiotemporal manner. Moreover, not only single cells but also single NAs<sup>61</sup> and single proteins<sup>62</sup> have been detected using this platform, demonstrating its versatility in the wide field of single-entity detection. In addition, the DMF system can be easily reconfigured between successive experiments and allows full automation of processing and detection on-chip.

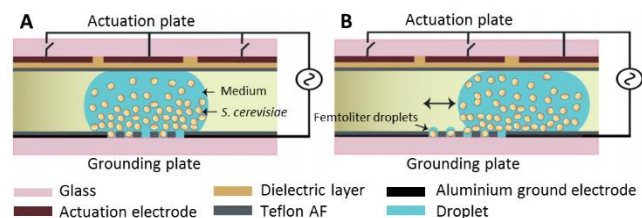


Figure 3. DMF microwell-based platform for single-cell toxicity studies. A) The DMF chip consisted of an actuation plate

and a grounding plate. The latter contained embedded microwells for cells to sediment. B) Following the sedimentation, the cells were actively seeded by shuttling the droplet back and forth over the array, which resulted in capturing a single cell per microwell. Adapted with permission from Ref.<sup>60</sup>. Published by The Royal Society of Chemistry.

### Single-cell NA analysis

The detection and analysis of NAs from single cells is relevant for understanding genotypic characteristics of individual cells<sup>63</sup>. This requires the release of the NAs through cell lysis and when performed on individual cells, entrapped within a small droplet or microchamber, this results in a high NA concentration<sup>31,64,65</sup>. To amplify the NA content even further and thus facilitate their detection and analysis, **droplet-based** microfluidic systems have been combined with polymerase chain reactions (PCR) on individual beads, termed emulsion PCR (ePCR)<sup>66,67</sup> (for more details, see section on single-NA detection). In this approach, a single cell is confined and lysed in a nL-sized droplet, containing a primer-functionalised microbead and PCR mixture. This allows generation of fluorescently labelled PCR amplicons on the beads and subsequent recovery of the bead from the emulsion for quantifying its fluorescence, thus enabling detection of specific genes in a simplex<sup>66</sup> or a multiplex<sup>67,68</sup> fashion (Figure 4). However, upon breaking of the emulsion, the beads carrying NA molecules from individual cells are mixed, losing thus a direct link with their originating cell. As a solution, advanced bar-coding techniques have been reported for the identification of individual RNA molecules from single cells<sup>69,70</sup>. Complex engineered primers, co-encapsulated with the single cells, enable to trace back each RNA molecule to its mother cell and even allow to identify the PCR duplicates of a single RNA molecule. This approach is currently being commercialised by 1CellBio (inDrop<sup>TM</sup>), 10x Genomics (GemCode) and recently also by Bio-Rad/Illumina (ddSEQ). Alternatively, single cells can be isolated in agarose droplets, which are cooled after PCR to obtain gelled droplets. These droplets, containing NA molecules of single cells, prevent mixing of the cell contents<sup>71–73</sup> next to facilitating DNA extraction and increasing the efficiency of PCR reactions<sup>46,63,74–75</sup>.

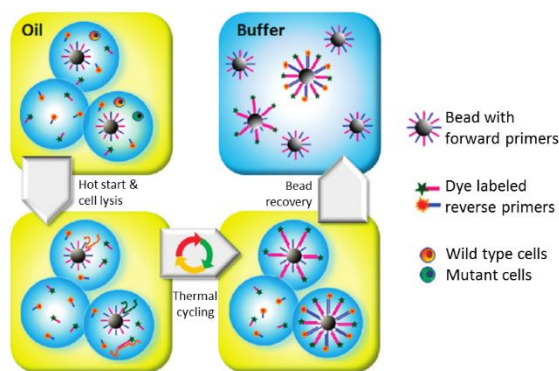


Figure 4. Multiplexed single-cell NA analysis using ePCR. First, primer-functionalised beads were co-encapsulated with single cells and a diluted PCR-mix. Subsequently, the cells



were lysed and thermally cycled to initiate PCR. Then, beads were recovered from the droplets and analysed by means of flow cytometry. Adapted with permission from Ref.<sup>67</sup>. Copyright 2010 American Chemical Society.

Alternatively, a fully integrated droplet-based DMF setup was reported by Rival *et al.* for single-cell RNA analysis based on reverse-transcription PCR (RT-PCR).<sup>76</sup> In this setup, an individual droplet containing a single cell was mixed on-chip with a second droplet, containing a lysis buffer and oligo-functionalised magnetic beads. Upon lysis, the released RNA was captured on the magnetic beads, which were subsequently washed and resuspended in a droplet, containing the RT-PCR mix. Following on-chip thermocycling, the generated RT-PCR amplicons were fluorescently detected, which enabled analysis of the genes expressed in the single cell. Although this DMF-based approach is not applicable for high-throughput analysis, contrary to the previously described droplet-based systems, the embedded thermocycling and the on-chip integration of all fluid manipulations allows full automation of single-molecule assays.

An example of a **microchamber**-based system for the analysis of NAs from single cells is the platform with electroactive microwells of Kobayashi *et al.*<sup>38</sup> (Figure 2), applied to detect specific DNA sequences on chromosomes of single cancer cells through fluorescent *in situ* hybridization. Next to this, many other platforms were reported, which are, however, out of the scope of this review as they are not integrated in microfluidic devices. Nevertheless, some of them show great potential for integration, such as the microarray-based systems for single-cell RT-PCR of the group of Love<sup>64</sup> and Dimov *et al.*<sup>77</sup>. In these PDMS-based platforms, single cells were seeded in 125 pL<sup>64</sup>- or 20 pL<sup>77</sup>-sized microwells through gravitational sedimentation and centrifugation, respectively, followed by adding RT-PCR reagents, sealing the microwells, lysing the cells and performing RT-PCR. The generated fluorescent signals were analysed to evaluate gene expression in single human B cells<sup>64</sup> and haematopoietic stem cells<sup>77</sup>. Although these microwell array setups required manual sample administration and array sealing, they could be fully automated through integration in a microfluidic chip. Furthermore, the same platforms have been modified to accommodate simultaneous detection of both NAs and secreted or surface-bound proteins from single cells, as detailed below.

### **Single-cell protein analysis**

In addition to using microfluidics for the study of the NA content of a single cell, microfluidic systems can also be applied for the analysis of proteins inside, secreted by or on the surface of a single cell, as described in the following sections.

#### **Analysis of intracellular proteins**

In order to evaluate the protein content of a single cell, cell lysis is generally required. However, there are some exceptions, as demonstrated by Huebner *et al.*<sup>78</sup>. They first reported a **droplet**-based platform for the direct detection

of a fluorescent protein, expressed in intact individual cells and later used a similar platform for the evaluation of alkaline phosphatase enzymes, expressed in single *E. coli* cells and accessible for fluorogenic substrate without disrupting the cell membrane<sup>79</sup>. Detection of the majority of intracellular proteins, however, does require lysis of the cell. For the evaluation of intracellular enzyme activity, this has been established in droplet-based systems by either co-encapsulating single cells with lysis buffer<sup>80</sup> or through rapid laser-induced lysis of droplet-encapsulated single cells<sup>81</sup>.

Besides droplet-based approaches, **microchamber**-based platforms have also been reported for the detection of intracellular proteins. For example, both Eyer *et al.*<sup>82</sup> and Xue *et al.*<sup>83</sup> developed a valve-based system in which microchambers were formed within parallel microfluidic channels by applying pressure on integrated valves (Figure 5). Although the number and size of these chambers was different between the 2 studies, in both approaches single cells were lysed and the target proteins were captured by antibodies, functionalised on the chamber surface, for their detection. Whereas the first system enabled detection of only 1 target at the time, the microchambers in the platform of Xue *et al.*<sup>83</sup> were functionalised with barcoded capture antibodies, enabling multiplex detection of up to 7 proteins and 4 metabolites from a single cell. The latter platform was furthermore applied for other single-cell applications, including the evaluation of protein-protein interactions<sup>84</sup> and the detection of proteins secreted by single cells (as explained further below)<sup>85</sup>. Although valve-based systems allow to address confined entities in a highly controlled way, the dimensions of the channels and integrated valves require larger sample volumes and limit the number of microchambers in a given area, hereby decreasing the throughput compared to droplet-based and other microchamber-based systems. Moreover, actuating multiple valves in complex patterns demands a precise and complex operation mechanism and requires a complex fabrication procedure. As an alternative, Park *et al.*<sup>86</sup> developed an easy-to-fabricate PDMS-based microfluidic chip with embedded microwells, in which single cells were trapped without the need for an external operation system, i.e. through capillary forces and a receding meniscus. Using this device, the response of single cells to the mating pheromone  $\alpha$ -factor was evaluated by monitoring the expression of green fluorescent protein. Additionally, to obtain a highly-efficient cell-seeding and thus enable the study of cell-sparse samples, the group of Herr<sup>87</sup> reported a centrifugation-driven lab-on-a-disc. In their microfluidic system, centrifugal forces were applied to isolate single cells in microwells, patterned in a polyacrylamide gel. Subsequently, the cells were lysed and the released proteins were subjected to electrophoretic separation through the wells into the surrounding gel, followed by single-cell western blotting. This approach enabled multiplexed detection of 4 different proteins starting from as few as 200 individual glioblastoma cells, contrary to other single-cell protein assays, requiring a starting population of thousands of cells<sup>87</sup>. Using a similar microwell-based western blot approach, they furthermore managed to simultaneously detect multiple

cytoplasmic and nuclear proteins of single cells through bi-directional electrophoresis, providing insight in single-cell protein signalling processes<sup>88</sup>. It should be noted that, contrary to the previously reported centrifugation-driven system, this microwell-based platform was not fully implemented in a microfluidic device.

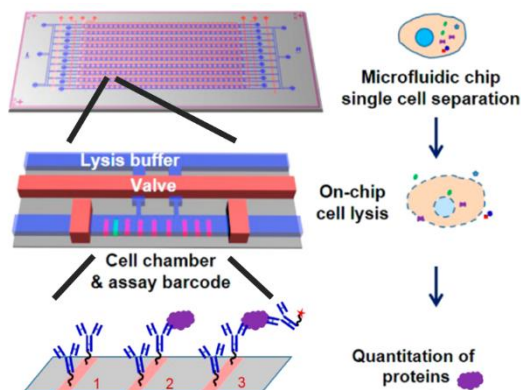


Figure 5. Valve-based microfluidic platform for the detection of intracellular proteins. Single cells were isolated in microchambers (310 chambers, 1.5 nL) formed by microvalves, which are positioned perpendicularly to the sample-containing microchannel. Upon cell lysis, intracellular proteins were captured on the prefunctionalized antibodies and subsequently detected through fluorescently labelled detection antibodies. The spatial separation of different capture antibodies in the barcode enabled multiplex protein detection. Adapted with permission from Ref.<sup>83</sup>. Copyright 2015 American Chemical Society.

### Analysis of secreted proteins

In contrast to intracellular protein analysis, which requires cell lysis, secreted proteins can be detected while the cell remains intact. In this context, Beneyton *et al.*<sup>89</sup> recently established a high-throughput **droplet**-based microfluidic system that allowed analysis of secreted recombinant enzymes from single yeast cells. In this approach, which resembles the one depicted in Figure 1, single cells were encapsulated in droplets of 20 pL, generated through flow-focusing at a rate of 3 000 droplets/second and followed by an off-chip growth step, reinjection in a second microfluidic device, addition of the fluorogenic substrate and analysis and sorting of the droplets based on their fluorescence at a rate of 300 droplets/second. The latter once more illustrates the discrepancy between the droplet generation and analysis throughput. Whereas this study mainly focused on the expression of hydrolytic enzymes, encoded from fungal genes, it can easily be translated to any other enzyme. Moreover, this platform is valuable for the selection of new enzymes by means of directed evolution or other protein engineering techniques. Alternatively, 2 similar droplet-based setups have been reported for the detection of secreted cytokines of single T-cells<sup>90</sup> and dendritic cells<sup>91</sup>. In both setups, single cells were co-encapsulated with beads that were functionalized with antibodies to specifically capture cytokines. These captured targets were subsequently labelled with fluorescently tagged detection antibodies and fluorescent droplets were

detected through flow cytometry<sup>90</sup> or fluorescence microscopy<sup>91</sup>. It should be noted that, in contrast to the majority of droplet-based platforms, where droplet analysis is performed in a fluidic flow, the droplets in the latter study were imaged after being immobilized in an incubation chamber, hosting up to 1 000 droplets at once. This approach introduces a discontinuity between the droplet generation and analysis throughput, with the latter being limited by the size of the incubation chamber and field of view of the detection system rather than the droplet-generation rate, similar to what was previously described for microchamber platforms. Moreover, the latter platform enabled monitoring of proteins on the surface of single dendritic cells, as well as their interactions with live T-cells, demonstrating the versatility of the approach<sup>91</sup>. Similar platforms have been described for the screening of effective antibodies, which are secreted by hybridoma cells and can be used for diagnostic or therapeutic purposes<sup>92,93</sup>.

Next to these droplet-based platforms, **microchamber** systems have been also reported for the detection of secreted proteins. One nice example is the above described valve-based platform of Xue *et al.* (Figure 5), which was also applied for multiplexed detection of various cytokines secreted by the isolated cells, showing its versatility towards different applications<sup>85</sup>. Although not integrated in a microfluidic platform, the promising PDMS-based microwell system of the group of Love, described above, was also used for the detection of cytokines and antibodies, secreted from single cells<sup>51,94–96</sup>. In their approach, cell-hosting microwells were sealed with an antibody-coated top-plate, which enabled localised capturing of the secreted proteins and was subjected to immuno-probing after disintegration from the chip. More recently, the versatility of this system was demonstrated by performing RT-PCR on the isolated single cells after analysis of their secreted products. By comparing the immune-probing and RT-PCR results of single wells, the correlation between protein secretion and gene expression in single human B cells could be evaluated<sup>64</sup>.

### Analysis of surface proteins

The last group of single-cell analysis techniques focusses on the detection of cell-surface proteins. Whereas highly- and moderately-abundant surface proteins can be detected through conventional flow cytometric techniques, detection of proteins that are present in low concentrations is more challenging as it not only requires protein labelling but also additional signal amplification. The latter has been carried out in confined volumes, enabling easy detection of the amplification product. In this context, 2 similar **droplet**-based platforms have been reported, relying on either enzymatic amplification<sup>97</sup> or Rolling Circle Amplification (RCA)<sup>98</sup>. In both platforms, the targeted surface proteins were first labelled by antibodies, followed by binding of a detection label ( $\beta$ -galactosidase ( $\beta$ gal) enzyme<sup>97</sup> and DNA primer<sup>98</sup>, respectively) and droplet encapsulation. These labels ensured the generation of an intense localized fluorescent signal only in those droplets with the targeted cells, enabling the detection of low-abundance surface proteins

on single monocytic cells<sup>97</sup> and individual cancer cells<sup>98</sup>. Whereas the throughput of droplet generation and analysis differed in the former study<sup>97</sup> (2 500 Hz and 1 500 Hz respectively), the droplets in the latter study<sup>98</sup> were analysed in an incubation chamber, hereby once more implying a discrepancy in the droplet generation and analysis throughput. A similar pL-droplet based platform has been described by Li *et al.*<sup>99</sup> for the detection of single-cell surface proteins through aptamer-based instead of antibody-based detection.

Proteins expressed on the surface of single cells have also been detected in **microchamber**-based platforms. For example, the previously described electroactive microwell-based platform of Kobayashi *et al.*<sup>38</sup> (Figure 2) was applied for the detection of cancer-related surface proteins as well, enabling discrimination of single cancer cells from individual white blood cells. More recently, the above described microwell-based platform of Dimov *et al.*<sup>77</sup> was adapted for

analysis of lung cancer-related surface proteins and simultaneous detection of their genetic expression in thousands of single cells (Figure 6)<sup>100</sup>, demonstrating the versatility of the system. In a first step, transmembrane cMET proteins were detected through fluorescent imaging of single cells, isolated in the 25 600 wells of the platform, after incubation with anti-cMET antibodies and fluorescently labelled secondary antibodies. Subsequently, the cells were lysed in their respective wells and their *cMET* mRNA expression was evaluated via RT-PCR, thus enabling to correlate surface protein and mRNA expression in single cells. This platform furthermore allowed to study the effect of transcription and translation inhibitors on protein and mRNA abundance, as well as the heterogeneous response of sensitive and resistant cell lines to cMET-targeting cancer therapeutics. Although integration in a microfluidic device was not reported and the initial array contained only 64 microwells, the platform shows great potential for high-throughput and automated single-cell gene and protein analysis.

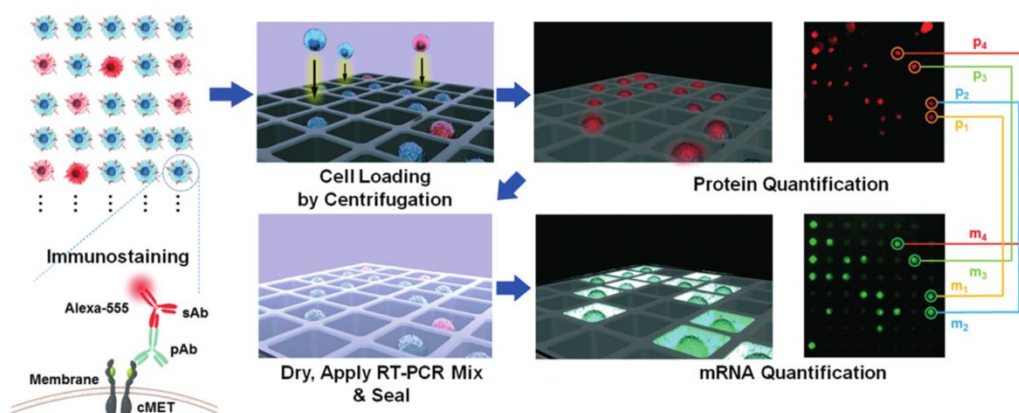


Figure 6. Microwell-based platform for simultaneous analysis of the expression of cell-surface proteins and genes. First, the immunostained single cells were loaded in the microwells by centrifugation and the targeted surface proteins were detected. After drying the array, the isolated cells were lysed and the intracellular mRNA of interest was detected through RT-PCR. Adapted from Ref.<sup>100</sup> with permission of The Royal Society of Chemistry.

## NUCLEIC ACID MOLECULES

DNA and RNA contain tremendous amounts of information as their involvement is a prerequisite in nearly every biological process, ranging from cell differentiation to aging. Unlocking this genetic data could be the key for gaining unique insights into various cell mechanisms, thereby contributing to the design of new, more accurate disease management strategies<sup>101</sup>. Therefore, developing techniques for the detection and analysis of single NA molecules has become extremely important. In the following paragraphs, an overview is provided on how target confinement within microfluidic devices can be used for single NA (1) detection, (2) sequencing and (3) stretching.

### Single-NA detection

A well-established technique for the detection of single NAs within individual containers relies on PCR-based am-

plification, for which a variety of systems have been reported and many are even commercially available. More recently, the major technical challenges of PCR are being tackled through the development of isothermal NA-amplification strategies and by enzymatically labelling the single NA molecules, thereby amplifying the fluorescent signal rather than the NAs, as described in the following sections.

### PCR-based amplification techniques

The conventional technique for detecting single NA molecules, termed digital PCR (dPCR), directly originated from the traditional PCR quantification. Whereas the latter is performed on multiple NA strands at once, in dPCR, single NA molecules are isolated in small containers where they are amplified individually by PCR and detected through fluorescent probes. Because of the large body of literature, we will focus only on those platforms that reached the stage of commercialization, with the exception of DMF-based and bead-based dPCR platforms (i.e. ePCR),

which are relatively new and not commercially available yet but worth discussing in the context of this review. For a more complete overview of all developed platforms, the interested reader is referred to the excellent review on the advances of dPCR by Cao *et al.*<sup>5</sup>.

Today, the most widely used approach for the encapsulation and detection of single NA molecules is the so-called **droplet** digital PCR (ddPCR)<sup>5,102–104</sup>. In this approach, each individual droplet contains either a single NA template or none, together with the necessary PCR components for subsequent amplification and detection of the confined molecules. Bio-Rad® used this technology to develop the QX100™ and QX200™, capable of generating approximately 20 000 droplets of 837 pL for the analysis of single NA molecules with a dynamic range of 5 orders of magnitude<sup>105,106</sup>. To increase the throughput and thus the dynamic range further, RainDance® commercialised RainDrop™ and, more recently, RainDrop Plus™, a ddPCR system that can produce up to 10 000 000 pL-sized droplets, enabling detection over 6 orders of magnitude<sup>105,107</sup>. Rare mutation detection and NA quantification are the main applications of these platforms<sup>108</sup>, which are mainly used in hospital laboratories (e.g. pathogen detection<sup>109</sup>, expression analysis<sup>110</sup> and cancer detection<sup>111</sup>). However, these commercial systems consist of 3 different devices for the successive generation of droplets, thermocycling for dPCR and fluorescent analysis of the droplets and thus require multiple sample transfer and processing steps. As a solution, Stilla Technologies recently launched the Naica system, enabling ddPCR with a single chip-loading step, using only 2 devices: the Naica Geode for combined droplet generation and thermocycling and the Naica Prism3 for 3-color readout<sup>112</sup>. Using this drastically simplified process, ddPCR can be performed in triplex in up to 30 000 droplets, over 5 orders of magnitude<sup>113</sup>.

Although not commercially available, the ultimate integration of ddPCR in a single system has been performed on a DMF platform (Table 1) by Norian *et al.*<sup>114</sup>. They developed a fully integrated DMF, enabling all key steps of PCR, including heating, transporting and fluorescent monitoring, on a single NA molecule isolated in an individual droplet of 1.2 nL. As proof-of-concept, they succeeded to detect a single copy of a NA strand, characteristic for *Staphylococcus aureus* and they furthermore were able to quantify the target DNA with a dynamic range of more than 4 orders of magnitude. Whereas the electronic circuits and the possibility of integrating all fluid manipulations on-chip make DMF-based ddPCR more convenient and allow for miniaturization and fully automated single-molecule assays, it poses difficulties in terms of high-throughput analysis, contrary to the conventional droplet-based platforms<sup>36,104</sup>.

To enable further analysis of NA amplicons in individual droplets after ddPCR, the ePCR concept was established with the co-encapsulation of primer-functionalized beads<sup>63,66,115</sup>. However, as stated before, when isolating single entities by diluting the sample, the vast majority of droplets contain no molecules, thus requiring analysis of a large number of droplets. Clearly, this becomes even more

problematic when co-encapsulating 2 different objects (e.g. DNA and bead), imposing a trade-off between throughput and accuracy<sup>103</sup>. Nevertheless, Shuga *et al.*<sup>115</sup> demonstrated the detection of a rare carcinogenic translocation in blood cancer using this approach. Similar to the setup depicted in Figure 4, single NA molecules were co-encapsulated into 2.5 nL droplets with primer-functionalised beads and a PCR mixture followed by ePCR. With this approach, the authors obtained an extremely low detection limit ( $< 1 \times 10^{-6}$  copies/genome) while maintaining the analysis efficiency and specificity. Furthermore, new clonal forms of the translocation were discovered, hereby paving the way to investigate the evolution of cancer<sup>115</sup>.

In addition to droplet-based approaches, dPCR has been also performed on **microchamber**-based microfluidic platforms. This has the advantage of compartmentalizing thousands of chambers in a single sealing step and performing the dPCR reactions in parallel, thus speeding up analysis time. A first platform, Constellation, was commercialised by Formulatrix and is based on the research of Vogelstein and Kinzler<sup>116</sup>, who were the first to implement a dPCR assay in the  $\mu$ L-sized wells of a 96-well plate. Today, these microplate formats have a smaller well-volume and an increased number of reaction chambers as each of the 96 wells contains 496 or more nL partitions at the bottom, which are connected through a microfluidic channel and can be sealed after loading the wells with the sample and PCR mixture (Figure 7)<sup>117</sup>. Hereby, single NA copies can be isolated in the partitions, enabling the visualization of individually amplified PCR products. This high-throughput approach enabled to analyse 96 samples at once and up to 384 samples per hour<sup>118</sup>.

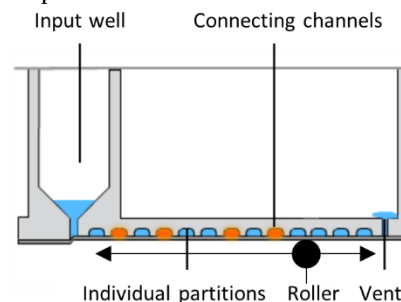


Figure 7. Side view of a single well of the Constellation dPCR setup. Each well contains hundreds of individual partitions at the bottom, which were loaded by forcing liquid from the input well into the connecting channels and were subsequently sealed, using a laminating roller along the bottom surface. Adapted with permission from Ref.<sup>117</sup>. Copyright 2014 Formulatrix.

An increase in throughput of dPCR in microchambers was achieved by introducing a valve-based platform, which resembles the system in Figure 5, and has been commercialised by Fluidigm under the name Biomark™. In this system, the sample and PCR premix are loaded into microfluidic channels, which are subsequently separated into microchambers by a NanoFlex™ valve (i.e. parallel structures, orthogonally placed to the microchannels). This way, com-



pletely independent micro-reaction chambers are obtained, in which the PCR reactions are carried out in parallel<sup>5,119–121</sup>. The system enables the isolation of individual NA molecules in up to 9 216 reaction chambers of 6.7 nL, resulting in a dynamic range of up to 6 orders of magnitude<sup>122</sup>. This has been used, among others, to perform multigene analysis of bacteria<sup>120</sup>, early diagnosis of cancer<sup>123</sup> and prenatal diagnosis<sup>124</sup>. An even higher throughput was achieved by performing dPCR on more advanced microwell array platforms, generally fabricated in silicon through photolithography<sup>118</sup>. Following this approach, Thermofisher® developed and commercialized its QuantStudio™ 3D Digital PCR system. The system consists of a chip, containing an array of 20 000 hexagonal wells of 0.8–1 nL for dPCR over 5 orders of magnitude<sup>5,125</sup>. This setup has proven its merits in several studies including cancer-related miRNA detection<sup>126</sup>, quantification of pathogens<sup>127</sup>, copy number variation detection<sup>128</sup> and mutation detection<sup>129</sup>.

### Isothermal amplification techniques

The applicability and integration of dPCR on microfluidic systems is hampered by the need for sophisticated thermal cycling instrumentation and space<sup>130</sup>. Isothermal amplification techniques bypass these limitations by amplifying the target at a constant reaction temperature, under simplified conditions and in less complex systems<sup>131</sup>. Because numerous of these isothermal amplification techniques for single NA detection have been developed in recent years, the majority of platforms are still in the research stages and thus not commercially available yet, in contrast to dPCR.

Rane *et al.*<sup>132</sup> and Mazutis *et al.*<sup>26</sup> developed a **droplet**-based platform for the isolation and isothermal amplification of single NA molecules. In these systems, the NAs were amplified through droplet-based loop-mediated isothermal amplification (dLAMP) and hyper-branched rolling circle amplification (HCRA) respectively, enabling digital quantification of the NAs. Moreover, in the latter platform, the amplified DNA was further analysed by adding an *in vitro* translation system, allowing to measure the enzymatic activity of the translated proteins. Schuler *et al.*<sup>133</sup> described another droplet-based platform in which a recombinase polymerase amplification (RPA) reaction was performed on single NA molecules. This reaction, which, in contrast to dLAMP and HCRA, does not require a DNA denaturation step, can proceed at temperatures between 37 and 42 °C<sup>134</sup> and results in 10<sup>4</sup>-fold amplification in 10 minutes. By integrating this droplet-based dRPA in a centrifugal microfluidic disk, the DNA of *Listeria monocytogenes* was quantified in only 30 minutes.

Isothermal amplification techniques for single-NA detection have been also implemented in **microchamber**-based platforms. For example, Gansen *et al.*<sup>135</sup> and Zhu *et al.*<sup>136</sup> integrated LAMP with the principle of limited dilution in a PDMS-based microwell array. Both systems furthermore enabled compartmentalization of the sample in the

wells without any mechanical operations by relying on inherent fluidic phenomena (i.e. the interplay between fluidic forces and interfacial tension)<sup>135</sup> or pre-stored energy (i.e. the pressure difference, generated by degassing the bulk PDMS)<sup>136</sup> respectively, thus requiring only limited to no external power. In another attempt for power-free single-NA compartmentalization, both Shen *et al.*<sup>137</sup> and Rodriguez-Manzano *et al.*<sup>138</sup> developed a SlipChip (Table 1) for performing RPA- and LAMP-based NA amplification, respectively. In these setups, 2 plates with embedded microchambers were aligned and brought in contact to create a fillable fluidic network. Upon sliding of the plates, individual nL-sized chambers were created where single NA molecules were isolated and thousands of isothermal amplification reactions were initiated in parallel. The first system was used for detecting single genomic DNA molecules of *Staphylococcus aureus*<sup>137</sup>. The second platform, combined with a variety of common cell phones as read-out system, demonstrated an affordable and pump-free system for quantification of the hepatitis C viral load. Alternatively, the commercially available valve-based Biomark™ system was applied by Blainey and Quake<sup>139</sup> to test the presence of DNA contamination in commercial protein preparations using multiple displacement amplification. This resulted in a limit of detection of 1 contaminating molecule per microliter, which is more sensitive than a conventional dPCR<sup>139</sup>.

### Enzyme-linked amplification techniques

Although PCR-based and isothermal amplification techniques are the most prevalent methods for the quantification of NAs<sup>23,140–144</sup>, they have several drawbacks such as quantification bias due to erroneous amplification of non-target sequences<sup>145,146</sup>. An alternative approach, circumventing this problem, is the indirect signal amplification by means of enzymes, turning a fluorogenic substrate into a measurable fluorescent product. As this technique does not rely on the replication of the NAs, no erroneous amplification of non-target sequences can occur, although other aspecific signals remain<sup>147</sup>. This concept is similar to the digital version of the well known enzyme-linked immunosorbent assay (ELISA), which will be addressed in more detail in the section on single-protein detection. It should be noted that the application of capture beads in these enzyme-linked amplification approaches enables to pre-concentrate a highly diluted sample before isolating the single molecules in confined volumes. This way, the number of confined volumes that must be interrogated to detect single targets decreases, providing the means to partially overcome the low concentration limit and thus decrease the detection limit of the platform.

Guan *et al.*<sup>140</sup> reported a **droplet**-based microfluidic approach for a digital enzyme-linked oligonucleotide hybridization assay (dELOHA) to detect single molecules of RNA (Figure 8). In this assay, an excess of magnetic beads with DNA capture probes was added to the RNA sample, allowing a single target RNA to hybridize to a single bead. Thereafter, enzyme-labelled ssDNA detection probes were hybridized to the RNA-DNA complex on the beads. Poisson statistics were applied a second time to encapsulate single,

enzyme-functionalised beads with the enzymatic substrate in pL droplets. These droplets were generated through flow-focusing on a PDMS-based chip, followed by in-line incubation of the emulsion and on-chip digital concentration readout. The performance of the platform was demonstrated by quantifying the *Neisseria gonorrhoeae* 16S rRNA in a clinical setting and the dELOHA was proven to be capable of quantifying DNA with a LOD of around 10 aM.

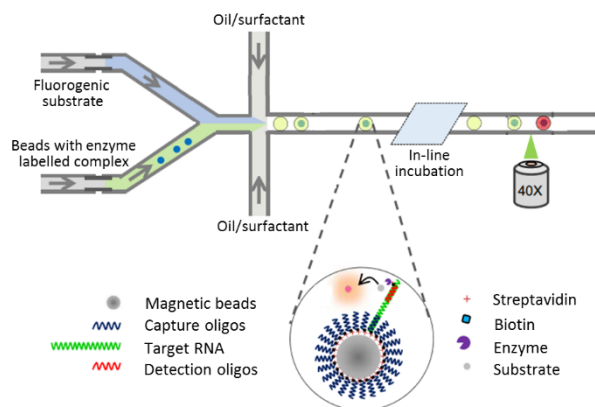


Figure 8. Droplet-based ELOHA for single NA detection. Single magnetic beads with an enzyme-labelled sandwich complex were co-encapsulated in a single droplet, together with the fluorogenic substrate. After on-chip incubation, the fluorescent signal of the droplets was analysed for the quantification of the target RNA. Adapted by permission from Macmillan Publishers Ltd: Scientific Reports (Ref.<sup>140</sup>), copyright (2015).

Alternatively, Song *et al.*<sup>147</sup> reported the detection of single DNA molecules in the fL-sized microwell arrays of the commercially available **microchamber**-based Simoa™ platform (for more details, see section on single-protein detection). In their approach, DNA molecules were incubated with detection probes and subsequently bound to paramagnetic beads, functionalized with capture probes. Next, the captured ssDNA was labelled with an enzyme and the bead-complexes were seeded via gravitational forces in fL-sized wells, together with the enzyme substrate. The resulting fluorescent signals allowed for a digital concentration readout of the original sample, which enabled the detection of *Staphylococcus aureus* genomic DNA in whole blood samples and river water. The obtained sensitivity of 10 aM<sup>147</sup> was comparable to the sensitivity of the previously described dELOHA. In addition to the Simoa™, the DMF-based microwell array platform, which was developed in our group (Figure 3), has been applied for the detection of single NA molecules through an enzyme-linked amplification<sup>61</sup>. Whereas the capturing and enzymatic labelling of single NAs on magnetic beads was performed in a similar fashion as on the Simoa™ platform, the bead-sample was transported over the wells through EWOD actuation instead of continuous microfluidics, enabling a highly flexible and reconfigurable droplet actuation. Using a magnet to attract the magnetic beads into the microwells moreover enabled to seed the beads with an unprecedented efficiency (98%), thus further addressing the low concentration limit. The developed platform was able

to quantify DNA from bacteria down to fM levels and was furthermore used to detect single proteins, as will be further elucidated in the section on single-protein detection.

### Single-NA sequencing

In order to obtain the most fundamental information of an NA strand, the precise order of the nucleotides (i.e. the sequence), has to be determined. Most NA sequencing methods rely on PCR-based amplification methods although direct sequencing is possible as well. Since there is a large body of literature on this topic, we will focus on the microfluidic platforms that reached the stage of commercialisation. Note that all commercial sequencing platforms apply **microchamber**-based confinement-techniques, as the sequential addition and extraction of nucleotides from individual droplets is challenging.

The first next-generation sequencing platform to be commercialised was 454 Sequencing. The device, initially brought to the market by Life Sciences and later by Roche, combined both droplet- and microwell-based confinement techniques (Figure 9)<sup>148</sup>. First, single NA templates were co-encapsulated with single beads in individual droplets to be amplified through ePCR. Next, the amplicon-carrying beads were retrieved from the droplets and seeded in individual optical fiber microwells. The sequence of the NA amplicons on the beads was then determined through pyrosequencing, generating light upon incorporation of a nucleotide. However, this setup had certain shortcomings, as the transfer of the beads to the microwells had to be performed manually and the pyrosequencing required multiple enzymes and optical scanning, turning it into a less automated and more costly approach. As such, over the years, 454 Sequencing lost its competitiveness with novel sequencing techniques and therefore, the manufacturer decided to stop the production in 2013.

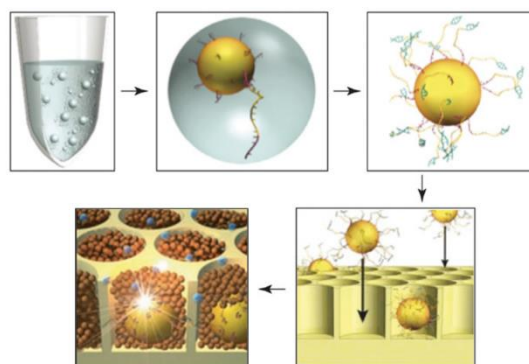


Figure 9. The working principle of 454 Sequencing. ePCR is followed by pyrosequencing in microwell arrays. Adapted by permission from Macmillan Publishers Ltd: Nature Biotechnology (Ref.<sup>148</sup>), copyright (2008).

Thermo Fisher Scientific distributed a second platform, called Ion Torrent™. It operates in a similar way as 454 Sequencing but is based on an electrochemical rather than an optical signal readout<sup>149,150</sup>. After ePCR, the beads are seeded in microwells, equipped with individual ISFET-

sensing elements. These sensors can detect single ions, released upon incorporation of a nucleotide, hereby determining the sequence of the bead-bound amplicons. Contrary to 454 Sequencing, the fully electronic detection system and lack of optical components turn this device into a low-cost, high-speed and high-throughput instrument.

A third platform is distributed by Pacific Biosciences, under the name Single Molecule Real Time (SMRT) sequencing. SMRT is based on the unique properties of a special kind of metal nanowell, called zero-mode waveguide<sup>151</sup>. Due to the size and shape of the waveguide, incident light of a certain wavelength decays exponentially, resulting in the illumination and thus observation of only a tiny spot in the well<sup>152</sup>. By immobilizing a DNA polymerase in that spot at the bottom of the waveguide and subsequently isolating a single DNA molecule in it, the incorporation of different fluorescently labelled nucleotides by the polymerase could be detected and hence the sequence of the target NA strand could be retrieved (Figure 10)<sup>151</sup>. The system is extremely high-throughput as a single coverslip can contain millions of zero-mode waveguide wells, resulting in massive parallelism<sup>152</sup>. Contrary to the previously described platforms, SMRT avoids to introduce sequence read biases through PCR and has long read lengths, which makes it suitable to obtain the sequence of entire genomes<sup>101</sup>.

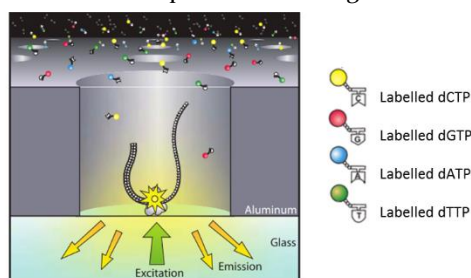


Figure 10. The confinement principle of SMRT sequencing of Pacific Biosciences. A DNA polymerase was enclosed in a single well, together with a single ssDNA template. Each well was illuminated from the bottom, with the zero-mode waveguide minimizing the focal spot of detection in which the incorporation of a fluorescently-labelled nucleotide was detected. Adapted from Ref.<sup>151</sup>. Reprinted with permission from AAAS.

### Single-NA stretching

Instead of uncovering the exact sequence of a single NA molecule, simply determining its length or combining this with a thorough labelling of the molecule (i.e. optical mapping) can also provide relevant fundamental information, reveal the identity of an organism or be used for diagnostic purposes<sup>101</sup>. However, NA molecules generally form a 3D “ball of wool” structure, hereby hampering length and even location analysis<sup>153</sup>. For that reason, single NA molecules must be confined in specialised structures to allow linearization or stretching, such as nanochannels, nanoslits and cross-slots (Table 1). Below, the different confinement approaches for NA stretching and related applications will be discussed.

One of the most commonly used **nanostuctures** for NA stretching are nanochannels<sup>154</sup>, which have been actively investigated for high-throughput and high resolution DNA analysis<sup>155</sup>. The major advantage of using nanochannels lies in its ability to linearize DNA to its full length without any knots or bumps, only as a result of the channel dimensions and the fluidic flow (Figure 11)<sup>156,157</sup>. Lam *et al.*<sup>158</sup> have developed a silicon nanofluidic chip containing around 4 000 nanochannels with a length of 0.4 mm and a diameter of 45 nm. Using this array of nanochannels, the authors could successfully stretch large bacterial artificial chromosomes and detect structural variations in the DNA, map the genome and use it as scaffold for next generation DNA sequencing. However, the main issue of these nanochannels is the difficulty in producing the small cross-sectional dimensions of the channel (45 nm). Nevertheless, they form the most frequently used approach for length analysis of DNA or DNA mapping and even have commercial applications (Irys<sup>®</sup> and Saphyr<sup>™</sup> technology of Bionanogenomics).

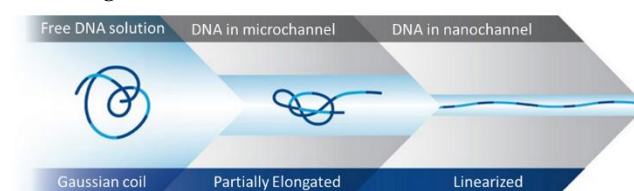


Figure 11. Nanochannel-based stretching of single NA molecules. DNA is elongated in a nanochannels due to the presence of confining walls. Adapted with permission from Ref.<sup>159</sup>. Copyright 2017 Bionanogenomics.

An interesting alternative to the 2D nanochannels are the 3D nanoslits, which are in essence very wide nanochannels that enable stretching of DNA in a planar way rather than linearly (Table 1). In contrast to nanochannels, nanoslits have been used for more theoretical applications, including the determination of specific DNA hydrodynamics or the evaluation of the influence of ionic strength on DNA stretching<sup>160,161</sup>. Moreover, nanoslits have been integrated in more complex setups for related applications, such as optical mapping, enabling for example the identification of DNA defects or disease-related genes. However, investigating a single DNA molecule at a time can be very time consuming. Therefore, Jo *et al.*<sup>162</sup> recently developed a high-throughput, PDMS-based device for optical DNA mapping, using a combination of microfluidic channels and nanoslits (Figure 12A). In this disposable platform, DNA was flown through the microchannels and, because of its dimensions in the relaxed state, did not diffuse into the nanoslits. However, upon activation of a lateral electric field, single molecules electrophoretically moved to and entered a nanoslit, resulting in progressive stretching and extension to its full length. The combination of aligning multiple nanoslits with a cheap and disposable chip made this an interesting concept for high-throughput optical DNA mapping.

In addition to optical mapping, there is nowadays more and more interest in the directed self-organisation of single



NA molecules. In this context, Reisner *et al.*<sup>163</sup> developed a microfluidic platform containing nanoslits, patterned with an array of very small nanopits (Figure 12B), which enabled to control the position and local conformation of single DNA molecules. In this system, single molecules were found to contain stretched areas within the nanoslits and relaxed areas in the nanopits. Whereas these nm-sized nanopits complicate the fabrication procedure, controlling the geometry of the nanopits enabled to guide the DNA in a specific manner over the surface and link specific points (i.e. pits) on the chip, which could be of great interest in, among others, the field of nanoelectronics.

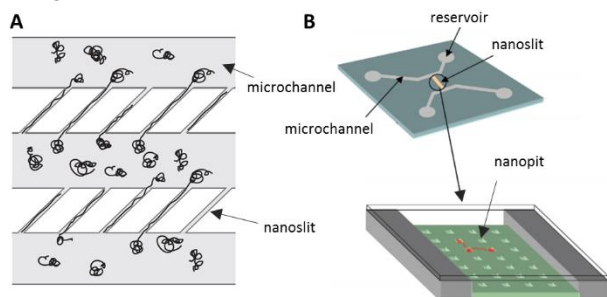


Figure 12. Applications for nanoslit-based NA stretching. A) Optical mapping using a PDMS microfluidic device which consisted of 2 parallel microchannels, connected by an array of aligned nanoslits, in which DNA was stretched. Adapted with permission from Ref.<sup>162</sup>. Copyright (2007) National Academy of Sciences, U.S.A. B) Directed self-organization using a microfluidic chip. The chip contained reservoirs for DNA and buffer storage. Between the 2 microchannels, a nanoslit was designed, containing an array of small nanopits (300x300 nm width, 100 nm depth). Adapted with permission from Ref.<sup>163</sup>.

The techniques, described above, focus on the stretching of single DNA molecules through structural confinement in nanochannels and nanoslits. Alternatively, DNA can be stretched in a so-called cross-slot (Table 1) by applying opposite flow forces<sup>161,164</sup>. In this setup, DNA is introduced into the cross-slot through the top lane while an ionic counter flow is generated from the opposite side through the bottom lane. If a DNA fragment arrives at the intersection, it can only be extended in the lateral direction and not towards the bottom or the top lane. When the counteracting flow forces are stopped, the DNA will relax back to its original state. This approach has the advantage that, although the microfluidic channels are relatively large (800  $\mu\text{m}$ ) and thus more easy to fabricate than nm-sized nanochannels, the actual confinement area is comparable, with the sidewalls formed by the opposing liquid flow. Moreover, the opposing liquid, flattening the DNA, can be easily exchanged, allowing detailed investigation of hazardous effects of chemicals or drugs on the folding or restriction of DNA<sup>164</sup> and even enabling single-molecule sequence detection, as shown by Dylla-Spears *et al.*<sup>165</sup>. In their PDMS-based cross-slot, single molecules were first stretched to their full length, followed by the successive addition of various sequence labels to the counteracting flow to fluorescently detect marker locations on the stretched DNA.

## PROTEINS

Proteins carry out a variety of functions, ranging from the transport of molecules to the facilitation of metabolic reactions in many crucial biological processes. Because of this, proteins are linked to various pathological conditions and can serve as biomarkers in diagnostics. Therefore, detection and analysis of individually confined protein molecules is of great interest in the field. In the following sections, approaches for the study and detection of (1) single enzymes and (2) single proteins will be discussed.

### Single-enzyme analysis

To study fundamental characteristics of individual enzyme molecules, Rotman<sup>166</sup> introduced already in the '60s the concept of isolating individual enzymes together with their fluorogenic substrate in a confined volume. This enabled single-enzyme detection with conventional microscopic techniques and revealed a large heterogeneity in single-enzyme kinetics<sup>166</sup>.

The potential of microfluidic **droplet**-based systems for single-enzyme studies was demonstrated 50 years after Rotman's initial report by Arayanarakool *et al.*<sup>167</sup>, who generated aqueous droplets (2.5-3  $\mu\text{m}$  diameter) of  $\beta$ -glucosidase molecules and fluorogenic substrate in a continuous oil phase, using a T-junction nanofluidic network. To increase the parallelization and throughput of these enzyme studies and thereby improve their sensitivity, Guan *et al.*<sup>168</sup> and Shim *et al.*<sup>169</sup> reported droplet-based microfluidic platforms in which respectively thousands of 4.2 pL droplets and millions of 10 fL droplets were generated per second by means of flow-focusing. By capturing the generated droplets in a monolayer, the fluorescence intensity of up to 200 000 droplets could be analyzed in parallel (Figure 13).

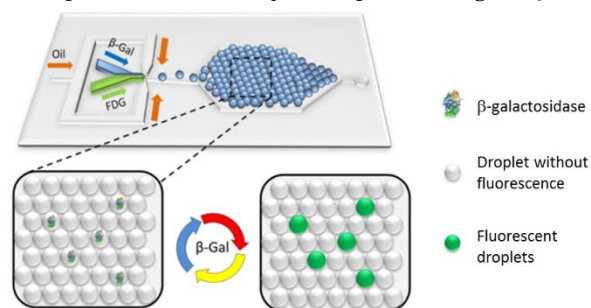


Figure 13. Droplet-based confinement of single enzyme molecules with an enlarged diagrammatic view of the droplet array and the enzymatic conversion of fluorogenic substrate to fluorescent product. Adapted from Ref.<sup>168</sup> with the permission of AIP Publishing.

Whereas droplet-based systems enable high-throughput detection of single enzyme molecules, a more thorough enzymatic study would require immobilization of the droplets to allow large-scale time-resolved analysis. This is resolved in **microchamber**-based systems, where the position of single molecules is inherently fixed. For example, the group of Walt applied their optical fiber microwell arrays, integrated into a PDMS-based microfluidic system



using an oil-sealing mechanism, to monitor the catalytic activity of single  $\beta$ gal molecules<sup>170</sup>. Besides optical fiber microwell arrays, microwells of varying dimensions were patterned into a PDMS surface for single-enzyme studies. For example, Jung *et al.*<sup>171</sup> integrated 100 fL-sized microwells (4.4  $\mu$ m diameter, 6.5  $\mu$ m depth) in a multilayer PDMS-based microfluidic device, enabling controlled and automated sealing of the wells by pushing the microchambers to the bottom of the microfluidic channel through a hydraulic pressure system. To overcome the need for external operating systems, Ota *et al.*<sup>172</sup> more recently developed a PDMS-based microfluidic device, using an immiscible liquid phase to enclose single  $\beta$ gal molecules and their substrate in thousands of 120 fL microchambers (5  $\mu$ m diameter, 6  $\mu$ m depth), built into the walls of a microfluidic channel (Figure 14A). In order to increase the throughput of these high-throughput microwell-based studies even further, the group of Noji micropatterned through-hole structures in a hydrophobic carbon-fluorin (CYTOP) layer on top of a glass slide. This way, over 10 000 000 hydrophilic-in-hydrophobic wells were generated at once<sup>173</sup>. After sequentially applying an aqueous enzyme solution and oil, dome-shaped droplets of the aqueous solution were retained on the exposed hydrophilic glass surface, while the hydrophobic surface remained covered with the oil (Figure 14B). Using this platform, the kinetics of single  $\beta$ gal and F1-ATPase molecules were studied<sup>173</sup>. More recently, the possibility to implement the microwell arrays in a microfluidic device was proven by assembling a flow cell, containing an access port for sample injection, on top of the microwell array<sup>174</sup>.

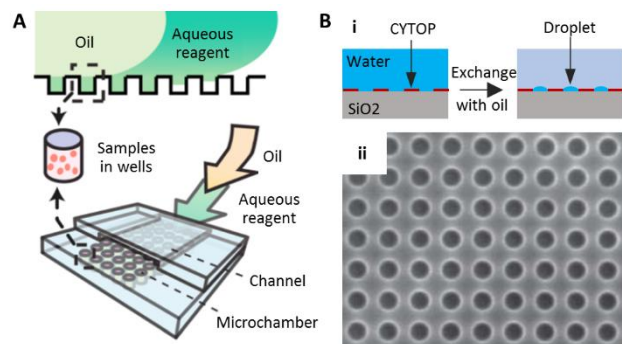


Figure 14. Confinement of single enzyme molecules in polymer-based microwell arrays, implemented in a continuous microfluidic platform. A) Schematic representation of target isolation in the microwells in the bottom-walls of a PDMS channel by sequentially flushing the aqueous reagent and an immiscible oil into the device. Adapted with permission from Ref.<sup>172</sup>. Copyright 2012 American Chemical Society. B) (i) Schematic representation of droplet retaining on a hydrophilic-in-hydrophobic micropatterned CYTOP surface and (ii) image of resulting array. Adapted from Ref.<sup>173</sup> with permission of The Royal Society of Chemistry.

### Single-protein detection

As stated above, the first reports on single-protein detection aimed at studying single-enzyme kinetics. In this context, it was also found that for low enzyme concentrations,

quantification could be obtained by digitally counting the number of active wells. Hence, this concept was applied for ultrasensitive protein detection by building enzyme-labelled immuno-complexes, similar to regular ELISAs, on microscopic beads and measuring them individually in confined reaction chambers. This approach, called digital ELISA (dELISA)<sup>175</sup>, outperforms the currently existing assays in terms of sensitivity as it reaches the ultimate single-protein resolution. It should be noted that target pre-concentration using capture beads enables to partially overcome the low concentration limit and increases the sensitivity of the platform, as was previously described in the section on single-NA detection.

Whereas **droplet**-based microfluidics are widely used for cell analysis and NA detection, only a limited amount of studies used this microfluidic approach for ultrasensitive protein detection. For example, the high-throughput droplet-based microfluidic platform of Shim *et al.*<sup>169</sup>, introduced in the section on single-enzyme analysis, was also employed for the detection of prostate-specific antigen (PSA) molecules. Single PSA molecules were captured on functionalised beads, followed by detection with a second antibody, labelling with an enzyme and subsequent encapsulation in fL droplets (Figure 15). The produced fluorescent signal was analysed by trapping the droplets in a monolayer, which could be flushed away in order to trap new droplets for sequential analysis. As such, a detection limit of 46 fM was obtained with an incubation time on-chip of only 10 min.

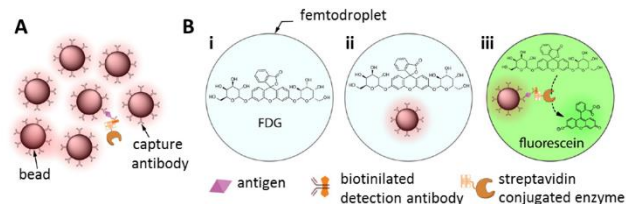


Figure 15. Ultrasensitive protein detection by confinement using droplet-based microfluidics. A) Formation of immuno-complexes on the antibody-coated beads, which were subsequently encapsulated in fL droplets with substrate and incubated on-chip. B) 3 types of droplets were generated: (i) droplets without a bead, (ii) droplets with a single bead but without the signal-generating immunocomplex and (iii) droplets with a bead and coupled immunocomplex, which generated a fluorescent signal through the  $\beta$ gal enzyme label. Adapted with permission from Ref.<sup>169</sup>. Copyright 2013 American Chemical Society.

Although the potential of droplet-based microfluidic systems for ultrasensitive protein detection has been demonstrated above, **microchamber**-based systems and microwell arrays, in particular, are more generally employed for this purpose (Table 1). Several types of microwell-based systems have been described in literature. The group of Walt, for example, reported on the use of their optical fiber microwell arrays for single PSA detection<sup>175</sup>. Here, the beads were trapped into the microwell array by centrifugation, reaching a seeding efficiency of 60 % after 10 minutes. More recently, the system was integrated

in a disk-based microfluidic device (Figure 16)<sup>176</sup> where vacuum pressure was applied to transport the target solution over the microwell array and the beads settled through gravity. This enabled a faster and more automated loading of the beads (60% seeding efficiency in 2 minutes) and sealing of the wells. Using this setup, PSA was detected with a detection limit of 400 aM and the concept was commercialised by the Quanterix Corporation under the name Simoa™ (Single Molecule Array). In addition to simplex detection, multiplex detection of 4 cytokines was demonstrated on this platform using subpopulations of beads, each with a unique fluorescent label, reaching a detection limit between 1.2 and 3.9 fM when spiked in buffer and plasma<sup>29</sup>. This is similar to simplex results and is, moreover, at least 10 times better when compared to conventional, analogue multiplex assays.

Another approach was reported by Kim *et al.*<sup>174</sup> who integrated the previously described CYTOP-based microwells (Figure 14B) in a PDMS-based microfluidic platform and combined this with prefunctionalised polystyrene beads. Following target capturing, the beads were trapped in the 65 fL-sized microwells by gravitation, followed by sealing with oil and resulting in a similar trapping efficiency (i.e. 60%) as reported above. However, the ability to analyse 1 000 000 microwells in parallel makes this platform highly sensitive, reaching a detection limit of 2 aM for PSA, which is around 20 times higher than the detection limits obtained with the optical fiber microwell arrays<sup>175</sup>.

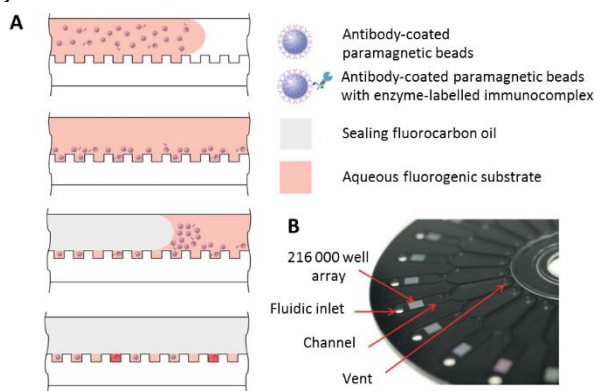


Figure 16. Ultrasensitive protein detection by confinement in microwell arrays, implemented in a microfluidic system. A) Schematic representation of a microwell-based setup that allowed bead trapping into microwells after capture of the target on the surface of the beads by sequentially flushing the aqueous bead-containing substrate solution and a sealing oil into the device. B) Picture of the disk-based microfluidic device, featuring fluidic channels and 24 arrays in total, each containing 216 000 microwells. Adapted from Ref.<sup>176</sup> with permission of The Royal Society of Chemistry.

In addition, our group reported the use of the DMF-based system (Figure 3) for confinement of single proteins in microwells<sup>62</sup>. In this study, single proteins were captured on prefunctionalised magnetic particles, after which they were manipulated on the DMF chip, allowing fully auto-

mated capture, seeding and analysis of single proteins inside the microwell array (62 500 microwells, 38 fL). Moreover, magnet-assisted trapping of the beads allowed to further reduce the low concentration limit by reducing the number of empty wells, as previously described. Using this platform, a detection limit of 10 aM was obtained for biotin-streptavidin interaction using  $\beta$ gal as a reporter enzyme, demonstrating a major step forward towards sensitive and fully automated single-molecule assays on-chip. Moreover, the same approach, although without full integration on the DMF platform, enabled the detection of influenza A nucleoprotein down to 10 fM in nasopharyngeal swabs<sup>177</sup> and Tau protein down to 55 aM in blood plasma<sup>178</sup>, illustrating once more the potential and versatility of this approach.

### Improvement of dynamic range

As mentioned in the previous section, the low concentration limit for single-protein detection has been partially overcome by increasing the throughput of the systems, pre-concentrating samples of low concentration with microbeads and improving the seeding efficiency of those beads in microwells. However, for high target concentrations, the chances of capturing multiple target molecules per bead increase according to Poisson statistics and thus digital counting becomes redundant. To overcome this high concentration limit and enlarge the dynamic range of digital assays, 2 different **microchamber**-based methods have been investigated.

The first method involves a combination of both digital and analogue readout and has been reported in 2 different formats. The first format, using optical fiber microwell arrays for a regular dELISA with advanced signal analysis, was presented by the group of Walt<sup>179</sup>. They performed digital and analogue counting on images with less and more than 70 % active wells, respectively (Figure 17A). Employing this strategy for the detection of PSA, they successfully extended the linear response from 2 orders of magnitude in the digital working range to over 4 orders of magnitude (250 aM to 3.3 pM). The second format, combining digital and analogue detection, was described by Piraino *et al.*<sup>180</sup>, using mechanically induced trapping of molecular interactions (MITOMI) in a valve-based system. The PDMS-based microfluidic platform contained 16 assay chambers which were formed by actuating valves or so called deflectable buttons in the chip. Half of those buttons were patterned with 484 wells (5  $\mu$ m diameter, 5  $\mu$ m depth) for digital readouts while the other half were flat buttons without microwells for analogue detection (Figure 17B). Using this setup, a dynamic range spanning at least 5 orders of magnitude (10 fM to 5 nanomolar (nM)) was obtained for the detection of GFP with only 5  $\mu$ L serum sample volume.

As an alternative for combining digital and analogue readouts, Ge *et al.*<sup>181</sup> reported a microwell-based platform with an extended dynamic range using the concept of Brownian trapping with drift (Figure 17C). The system consisted of a microfluidic channel with embedded microwells, which were grouped into parallel regions and

contained beads, functionalized with capture reagents. Upon addition of the sample, target molecules were captured in the wells, followed by a labelling and sealing step. For low target concentrations, most molecules were trapped in the beginning of the channel (i.e. Region 1) and with less than 80 % of the wells being active (i.e. captured at least 1 molecule), the target could be quantified using conventional Poisson statistics. For exponentially increasing concentrations, however, target molecules were also trapped in the downstream regions and the region with

less than 80% active wells was found to shift downstream linearly. By relating the digital signal in that region with its location, the sample concentration could be derived. The performance of the approach was analysed in a clinical matrix for the detection of TNF- $\alpha$  in 25 % serum, revealing a total dynamic range of over 5 orders of magnitude (6 fM to 2 nM). This was slightly wider than the dynamic range obtained by combining the digital and analogue readout as shown by Rissin *et al.*<sup>179</sup> and Piraino *et al.*<sup>180</sup>.

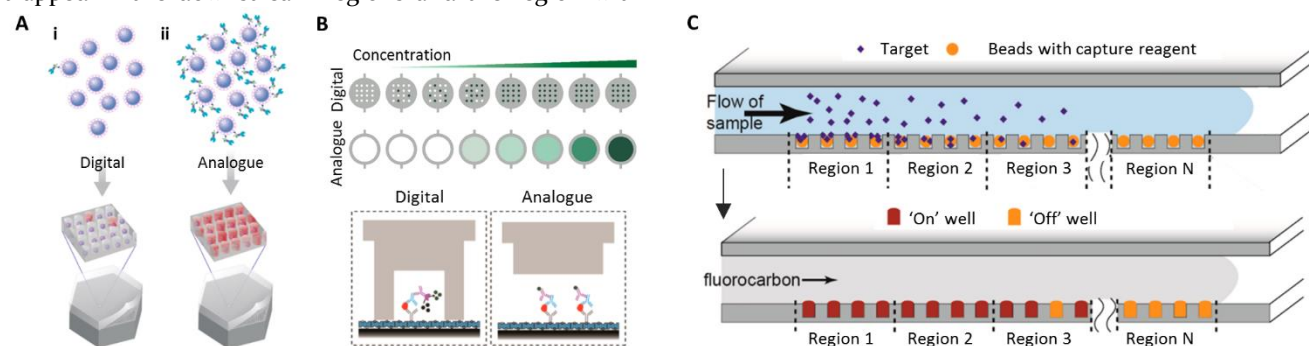
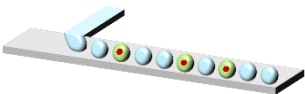
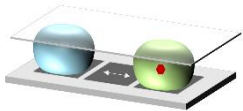
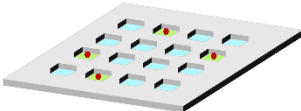
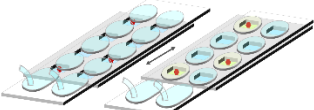
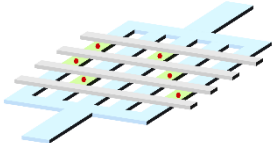
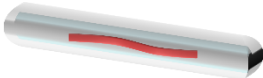
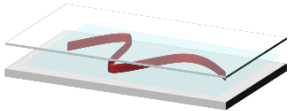
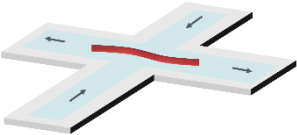


Figure 17. Improving the dynamic range of digital assays. A) Schematic representation of the microwell-based combination of digital (i) and analogue (ii) readouts. Adapted with permission from Ref.<sup>179</sup>. Copyright 2011 American Chemical Society. B) Schematic representation of the MITOMI-based combination of analogue and digital readout by implementation of 2 compartments (i.e. 1 for analogue and 1 for digital detection) in the assay chamber. Adapted with permission from Ref.<sup>180</sup>. Copyright 2016 American Chemical Society. C) Schematic representation of the microwell-based system using Brownian trapping with drift. While the sample flowed through the channel with embedded microwells, target molecules were captured on the beads, trapped in the microwells. Evaluating the spatial distribution of active (i.e. 'on') microwells enabled to perform digital quantification with a large dynamic range. Adapted with permission from Ref.<sup>181</sup>. Copyright 2014 American Chemical Society.

**Table 1. Overview of the main confinement strategies in this review, with an indication of the applied field, combined with references of selected papers and the related commercially available devices.**

Confinement strategy	Confinement type	Schematic representation	Application field + Selected references	Commercial devices
Droplets	CMF-based		S-cell detection <sup>37,39</sup> , S-cell NA analysis <sup>66–68,71–73</sup> , S-cell protein analysis <sup>78–81,89–91,97,98</sup> S-NA detection <sup>109–111</sup> , S-NA sequencing <sup>148</sup> S-enzyme analysis <sup>167–169</sup> , S-protein detection <sup>169</sup>	inDrop™, GemCode, ddSEQ, RainDrop™, Qx100™, Qx200™, Naica™
	DMF-based		S-cell NA analysis <sup>76</sup> S-NA detection <sup>114</sup>	None reported
Microchambers	Microwell-based		S-cell detection <sup>38,58,60</sup> , S-cell NA analysis <sup>38</sup> , S-cell protein analysis <sup>38,86</sup> S-NA detection <sup>62,126,135,136,147</sup> , S-NA sequencing <sup>148,151</sup> S-enzyme analysis <sup>170–172</sup> , S-protein detection <sup>62,174,176,179,181</sup>	Constellation, QuantStudio™, 454 Sequencing, Ion Torrent™, SMRT, Simoa™
	Slipchip-based		S-NA detection <sup>137,138</sup>	None reported
	Valve-based		S-cell protein analysis <sup>82,83,85</sup> S-NA detection <sup>120,139</sup> S-protein detection <sup>180</sup>	Biomark™
Nanostructures	Nanochannel-based		S-NA stretching <sup>158</sup>	Irys®, Saphyr™
	Nanoslit-based		S-NA stretching <sup>162,163</sup>	None reported
	Cross-slot-based		S-NA stretching <sup>165</sup>	None reported



## SUMMARY AND OUTLOOK

---

In this review, we highlighted the recent advances in the field of single-entity detection in confined volumes within microfluidic devices. Contrary to the conventional ensemble measurements, single-entity approaches enable the examination of individual entities within an entire population and enable detection of targets in the low fM or even aM range. Because of these promising features, single-entity detection techniques are currently becoming the focus of attention both for fundamental biological studies as well as for the diagnostic field.

Whereas various single-entity approaches have been reported over the last decades, we put special emphasis on those that rely on physical target confinement in small volumes. We believe that they offer immense potential as they enable high-throughput and parallelized detection of single targets while their implementation in microfluidic devices furthermore improves their potential by (i) allowing for miniaturization, (ii) lowering the sample volume, reagents requirements and the reaction time and (iii) increasing the automation.

As indicated in (Table 1) some of the reported confinement strategies are highly versatile in terms of the target entities, whereas others are not. We found nanostructures to be limited to NA-related studies, as they are specifically tailored for single-NA stretching, whereas droplet-based and microchamber-based platforms can be used for a wide range of targets (i.e. cells, NAs and proteins). Nevertheless, the latter 2 confinement strategies have specific characteristics, which are beneficial in different applications. For example, droplet-based systems can be used for the isolation of both adherent and non-adherent cells, whereas microchamber-based platforms generally have to be treated with adhesive proteins to enable trapping of non-adherent cells. On the other hand, long-term studies of single entities can be more easily performed in microchambers because of their inherently fixed position, whereas droplet-based systems only allow for time-resolved measurement when their location can be tracked. Nevertheless, several highly versatile droplet- and microchamber-based platforms have been reported to be easily exchangeable between targets and applications.

In addition to their versatility, the reported confinement strategies differ in the need for and complexity of external components, required for their operation and readout. For example, valve-based systems depend on complex controlling systems in order to operate the valves in a precise and structured way and to offer proper control over single entities, whereas SlipChips enable isolation of single entities in microchambers by simply sliding 2 plates across each other. Alternatively, droplet-based and microwell-based platforms generally require the operation of pumps and valves, although power-free microwell-based systems, relying on pre-stored energy or inherent fluidic phenomena only, have been reported as well. Lastly, the electronic circuits, required for DMF-based platforms, can be operated

with a minimal amount of power and enable miniaturization and integration of multiple assay-steps on-chip, hereby reducing the external components in general and improving in particular the automation-potential of single-entity platforms. In terms of the readout instrumentation, droplet-based platforms were found to be limited to remote, optical readout systems, either analysing a single droplet at a time or multiple droplets at once in a collection chamber. Microchamber-based systems, on the other hand, allow both remote and ‘invasive’ sensing of multiple confined volumes at once, without compromising their integrity and thus are complementary with optical as well as electrochemical readout systems. This enables the use of fully electronic detection systems, lowering the cost while increasing the speed and throughput.

As indicated in the review, also the fabrication process of the reported single-entity confinement strategies differs in complexity. Whereas droplet-, microwell- and SlipChip-based platforms with  $\mu\text{m}$ -dimensions are generally fabricated through conventional lithography or etching procedures, the fabrication of nanochannels and nanoslits is more challenging due to their nm-dimensions, required for the stretching of single NA molecules. The production of cross-slots, on the other hand, is less demanding as their overall dimensions are in the  $\mu\text{m}$ -range, which can be achieved with conventional techniques, whereas their confinement area, formed at the intersection of the counter-acting flows, is comparable to that of a nanochannels. The fabrication of valve-based systems, lastly, is rather complex because of the need for a multi-layer system with highly controllable valves and advanced operating systems.

Various confinement-based platforms have been reported for the research purposes of all 3 target types mentioned in this review. However, most commercially available single-entity confinement techniques focus on detecting single NA molecules (Table 1). This can be explained partly by the general stimulus in DNA research in the past decade and the increased interest in genetics for medical applications. However, nowadays, with the advancements in microfluidics and microfabrication techniques, the field of single-cell and single-protein detection is rapidly evolving and commercial applications for their detection start to find their way to the market.

Although single-entity studies have improved drastically over the last decade, there are still a few challenges that need to be addressed. The first challenge is the low concentration limit, which plays a crucial role in the low dynamic range. This limit is based on the fact that at low sample concentrations, a high number of confined volumes have to be imaged before a single entity will be detected, as a large amount of the confined volumes remains empty. As highlighted in this review, recent research has either tried to deal with this issue by increasing the throughput and parallelization level of the systems or tried to overcome it by decreasing the number of empty droplets or wells. Attempts to increase the throughput were especially successful for CMF droplet-based and microwell-based systems, as their throughput both improved from tens to thousands of confined volumes per second or at once. Note

that, when evaluating the throughput of a system, one should consider the number of single volumes that can be analysed at a certain rate or in parallel, rather than their confinement rate. For example, whereas improvements in microfluidic techniques enable the generation of millions of droplets per second, the detection system might enable analysis of the droplets at a lower rate only or might require the droplets to be collected in an incubation chamber and analysed with only a few thousand at once. Similarly, whereas recent microfabrication techniques allow to generate microwell arrays with millions of embedded wells, the field-of-view of the detection mechanism might enable analysis of only a few thousand volumes in parallel, thus decreasing the true throughput of the system. As such, the detection approach (i.e. serial or parallel detection of confined volumes) plays a major role in overcoming the low concentration limit and thus in increasing the dynamic range. Nevertheless, CMF droplet-based and microwell-based platforms enable the highest throughputs when compared to SlipChips and especially valve-based systems, the latter limited by the dimensional and structural requirements of the valves and channels. DMF droplet-based platforms also have a limited throughput, as a DMF platform enables the manipulation and analysis of 1 or only a few droplets at once, each confining a single entity. In contrary, the recent integration of a microwell array on a DMF-based platform has proven its potential for single-entity studies as it combines the massive throughput and automation-potential of the respective technologies. As previously mentioned, in addition to increasing the throughput, other attempts to overcome the low concentration limit focussed at decreasing the number of empty droplets or wells in the platform. The latter was established by, for example, aligning the entities in an evenly spaced, ordered stream before encapsulation in droplets, actively seeding single entities in microwells through electrophoretic forces or pre-concentrating single entities on beads, which was even further improved through magnet-assisted trapping of those beads in microwell arrays.

It should be noted that the low concentration limit is directly related to the sensitivity of a system, as the lowest target concentration that can be detected is directly related to the number of volumes that can and have to be analysed before detecting a single entity. However, sensitivity is not a crucial factor in all applications reported in this review. Whereas the study of single-cell behaviour, single-NA stretching or single-enzyme kinetics in cellular and molecular biology does require the isolation of single entities, this is generally not done from a low-concentration sample. In contrary, detection of low concentrations of, for example, protein or NA biomarkers in diagnostics requires extreme detection limits and thus benefits from the strategies, developed to overcome the low concentration limit. This is nicely illustrated by the large number of publications on single-NA and single-protein detection in CMF droplet-based and microwell-based platforms (Table 1), for which the majority of these strategies have been developed.

Another challenge for single-entity studies is the high concentration limit, the second factor impacting the dynamic range. This limit states that, at high sample concentrations, the possibility to detect a single entity decreases as the chance of isolating more than 1 entity in the confined volume increases. Thus, research has been striving to overcome the high concentration limit and thus improve the dynamic range by, for example, combining a digital and analogue readout on the same platform or by relying on the spatial decaying distribution of molecules, trapped in a successive regions of a microwell-based platform. Again, it should be noted that these improvements in dynamic range are especially relevant in medical diagnostics with various disease biomarkers being present in a wide range of concentrations.

A third challenge in the field is the simultaneous detection of different single entity molecules in a single test. Only some of the included studies reported multiplexed single-entity studies in microfluidic platforms so far. However, we believe that the majority of platforms have multiplex-capabilities and that future research would allow to reveal the true potential of this approach for both the molecular biology and diagnostic field. This could for example provide revolutionary new insights in biological processes such as the progression of diseases or enable the simultaneous detection of multiple biomarkers, related to 1 or multiple disorders, to speed up the currently available diagnostic tests and improve their performance.

In conclusion, microfluidic-based platforms for single-entity detection in solitary confinement offer huge benefits, not only as a biological research tool but also as biosensors for medical diagnostic purposes. Microfluidic and microfabrication approaches have and will continue to be improved in order to increase the throughput and decrease the power and external components, required for the operation of these systems, all with the aim to automate and miniaturise high-throughput single entity studies. Although it is hard to fully envision what the future holds, we predict a wide expansion of their commercial availability.

## ACKNOWLEDGEMENTS

The research leading to this review has received funding from KU Leuven (OT 13/058, C3 2/15/005, PDM 17-093), Research Foundation–Flanders (FWO Go86114N, Go80016N, SB/1S30016N, SB/1S30116N, SB/1S32217N) and VLK (C8744). This project has received funding from the European Union’s Horizon 2020 research and innovation programme under the Marie Skłodowska-Curie grant agreement No 675412 (H2020-MSCA-ITN-ND4ID) and No 764281 (H2020-MSCA-ITN-AiPBAND). The research leading to these results has received funding from the European Research Council under the European Union’s Seventh Framework Programme (FP/2007-2013)/ERC Grant Agreement (Grant No. 291593).

## REFERENCES

- (1) Xie, Z.; Srividya, N.; Sosnick, T. R.; Pan, T.; Scherer, N. F. Single-Molecule Studies Highlight Conformational Heterogeneity in the Early Folding Steps of a Large Ribozyme. *Proc. Natl. Acad. Sci.* **2004**, *101* (2), 534–539.
- (2) Ziemba, B. P.; Li, J.; Landgraf, K. E.; Knight, D.; Voth, G. A.; Falke, J. J. Single-Molecule Studies Reveal a Hidden Key Step in the Activation Mechanism of Membrane-Bound Protein Kinase C- $\alpha$ . *Biochemistry* **2014**, *53*, 1697–1713.
- (3) Altschuler, S. J.; Wu, L. F. Cellular Heterogeneity: When Do Differences Make a Difference? *Cell* **2010**, *141* (4), 559–563.
- (4) Schubert, C. The Deepest Differences. *Nature* **2011**, *480* (7375), 133–137.
- (5) Cao, L.; Cui, X.; Hu, J.; Li, Z.; Choi, J. R.; Yang, Q.; Lin, M.; HuiLi, Y.; Xu, F.; Hui, L. Y.; Xu, F. Advances in Digital Polymerase Chain Reaction (dPCR) and Its Emerging Biomedical Applications. *Biosens. Bioelectron.* **2017**, *90*, 459–474.
- (6) Xie, X. S.; Dunn, R. C. Probing Single Molecule Dynamics. *Science* **1994**, *265* (5170), 361–364.
- (7) Craig, D. B.; Arriaga, E.; Wong, J. C. Y.; Lu, H.; Dovichi, N. J. Life and Death of a Single Enzyme Molecule. *Anal. Chem.* **1998**, *70* (1), 39A–43A.
- (8) Pérez-Ruiz, E.; Kemper, M.; Spasic, D.; Gils, A.; Van Ijzendoorn, L. J.; Lammertyn, J.; Prins, M. W. J. Probing the Force-Induced Dissociation of Aptamer-Protein Complexes. *Anal. Chem.* **2014**, *86* (6), 3084–3091.
- (9) Pérez-Ruiz, E.; Spasic, D.; Gils, A.; van Ijzendoorn, L. J.; Prins, M. W. J.; Lammertyn, J. Ara H 1 Protein-Antibody Dissociation Study: Evidence for Binding Inhomogeneities on a Molecular Scale. *N. Biotechnol.* **2015**, *32* (5), 458–466.
- (10) Walt, D. R. Optical Methods for Single Molecule Detection and Analysis. *Anal. Chem.* **2013**, *85* (3), 1258–1263.
- (11) Landegren, U.; Vänellid, J.; Hammond, M.; Nong, R. Y.; Wu, D.; Ulleras, E.; Kamali-Moghaddam, M. Opportunities for Sensitive Plasma Proteome Analysis. *Anal. Chem.* **2012**, *84*, 1824–1830.
- (12) Eiger, M.; Rigler, R. Sorting Single Molecules: Application to Diagnostics and Evolutionary Biotechnology. *Proc. Natl. Acad. Sci. USA.* **1994**, *91*, 5740–5747.
- (13) Todd, J.; Freese, B.; Lu, A.; Held, D.; Morey, J.; Livingston, R.; Goix, P. Ultrasensitive Flow-Based Immunoassays Using Single-Molecule Counting. *Clin. Chem.* **2007**, *53* (11), 1990–1995.
- (14) Müller, S.; Nebe-von-caron, G. Functional Single-Cell Analyses: Flow Cytometry and Cell Sorting of Microbial Populations and Communities. *FEMS Microbiol Rev* **2010**, *34* (4), 554–587.
- (15) Tessler, L. A.; Reifengerger, J. G.; Mitra, R. D. Protein Quantification in Complex Mixtures by Solid Phase Single-Molecule Counting. *Anal. Chem.* **2009**, *81* (17), 7141–7148.
- (16) Wang, X.; Gou, X.; Chen, S.; Yan, X.; Sun, D. Cell Manipulation Tool with Combined Microwell Array and Optical Tweezers for Cell Isolation and Deposition. *J. Micromechanics Microengineering* **2013**, *23*, 75006.
- (17) Decrop, D.; Brans, T.; Gijzenbergh, P.; Lu, J.; Spasic, D.; Kokalj, T.; Beunis, F.; Goos, P.; Puers, R.; Lammertyn, J. Optical Manipulation of Single Magnetic Beads in a Microwell Array on a Digital Microfluidic Chip. *Anal. Chem.* **2016**, *88* (17), 8596–8603.
- (18) Li, L.; Chen, S.; Oh, S.; Jiang, S. In Situ Single-Molecule Detection of Antibody - Antigen Binding by Tapping-Mode Atomic Force Microscopy. *Anal. Chem.* **2002**, *74* (23), 6017–6022.
- (19) Armani, A. M.; Kulkarni, R. P.; Fraser, S. E.; Flagan, R. C.; Vahala, K. J. Label-Free, Single-Molecule Detection with Optical Microcavities. *Science* **2007**, *317*, 783–787.
- (20) Gooding, J. J. Nanoscale Biosensors: Significant Advantages over Larger Devices? *Small* **2006**, *2* (3), 313–315.
- (21) Chang, L.; Rissin, D. M.; Fournier, D. R.; Piech, T.; Patel, P. P.; Wilson, D. H.; Duffy, D. C. Single Molecule Enzyme-Linked Immunosorbent Assays: Theoretical Considerations. *J. Immunol. Methods* **2012**, *378* (1–2), 102–115.
- (22) Holzmeister, P.; Acuna, G. P.; Grohmann, D.; Tinnefeld, P. Breaking the Concentration Limit of Optical Single-Molecule Detection. *Chem. Soc. Rev.* **2014**, *43* (4), 1014–1028.
- (23) Streets, A. M.; Huang, Y. Microfluidics for Biological Measurements with Single-Molecule Resolution. *Curr. Opin. Biotechnol.* **2014**, *25*, 69–77.
- (24) Gooding, J. J.; Gaus, K. Single-Molecule Sensors: Challenges and Opportunities for Quantitative Analysis. *Angew. Chemie - Int. Ed.* **2016**, *55*, 11354–11366.
- (25) Walt, D. R. Protein Measurements in Microwells. *Lab Chip* **2014**, *14*, 3195–3200.
- (26) Mazutis, L.; Araghi, A. F.; Miller, O. J.; Baret, J. C.; Frenz, L.; Janoshazi, A.; Taly, V.; Miller, B. J.; Hutchison, J. B.; Link, D.; Griffiths, A. D.; Ryckelynck, M. Droplet-Based Microfluidic Systems for High-Throughput Single DNA Molecule Isothermal Amplification and Analysis. *Anal. Chem.* **2009**, *81* (12), 4813–4821.
- (27) Basu, A. S. Digital Assays Part I: Partitioning Statistics and Digital PCR. *SLAS Technol.* **2017**, *22* (4), 369–386.
- (28) Basu, A. S. Digital Assays Part II: Digital Protein and Cell Assays. *SLAS Technol.* **2017**, *22* (4), 387–405.
- (29) Rissin, D. M.; Kan, C. W.; Song, L.; Rivnak, A. J.; Fishburn, M. W.; Shao, Q.; Piech, T.; Ferrell, E. P.; Meyer, R. E.; Campbell, T. G.; Fournier, D. R.; Duffy, D. C. Multiplexed Single Molecule Immunoassays. *Lab Chip* **2013**, *13* (15), 2902–2911.
- (30) Whitesides, G. M. The Origins and the Future of Microfluidics. *Nature* **2006**, *442* (7101), 368–373.
- (31) Najah, M.; Griffiths, A. D.; Ryckelynck, M. Teaching Single-Cell Digital Analysis Using Droplet-Based Microfluidics. *Anal. Chem.* **2012**, *84* (3), 1202–1209.
- (32) Squires, T. M.; Quake, S. R. Microfluidics: Fluid Physics at the Nanoliter Scale. *Rev. Mod. Phys.* **2005**, *77* (3), 977–1026.
- (33) Tang, M.; Wang, G.; Kong, S. K.; Ho, H. P. A Review of Biomedical Centrifugal Microfluidic Platforms. *Micromachines* **2016**, *7* (2), 26.
- (34) Seemann, R.; Brinkmann, M.; Pfohl, T.; Herminghaus, S. Droplet Based Microfluidics. *Reports Prog. Phys.* **2012**, *75* (1), 41.
- (35) Choi, K.; Ng, A. H. C.; Fobel, R.; Wheeler, A. R. Digital Microfluidics. *Annu. Rev. Anal. Chem.* **2012**, *5* (1), 413–440.
- (36) Kokalj, T.; Pérez-Ruiz, E.; Lammertyn, J. Building Bio-Assays with Magnetic Particles on a Digital Microfluidic Platform. *N. Biotechnol.* **2015**, *32* (5), 485–503.
- (37) Pan, J.; Stephenson, A. L. L.; Kazamia, E.; Huck, W. T. S. T.; Dennis, J. S. S.; Smith, A. G. G.; Abell, C. Quantitative Tracking of the Growth of Individual Algal Cells in Microdroplet Compartments. *Integr Biol* **2011**, *3* (10), 1043–1051.
- (38) Kobayashi, M.; Kim, S. H.; Nakamura, H.; Kaneda, S.; Fujii, T. Cancer Cell Analyses at the Single Cell-Level Using Electroactive Microwell Array Device. *PLoS One* **2015**, *10* (11), 1–10.
- (39) Brouzes, E.; Medkova, M.; Savenelli, N.; Marran, D.; Twardowski, M.; Hutchison, J. B.; Rothberg, J. M.; Link, D. R.; Perrimon, N.; Samuels, M. L. Droplet Microfluidic Technology for Single-Cell High-Throughput Screening. *Proc. Natl. Acad. Sci.* **2009**, *106* (34), 14195–14200.
- (40) Zhang, Q.; Wang, T.; Zhou, Q.; Zhang, P.; Gong, Y.; Gou, H.; Xu, J.; Ma, B. Development of a Facile Droplet-Based Single-Cell Isolation Platform for Cultivation and Genomic Analysis in Microorganisms. *Sci. Rep.* **2017**, *7* (41192), 11.
- (41) Schmitz, C. H. J. H. J.; Rowat, A. C. C.; Köster, S.; Weitz, D. A. Dropspots: A Picoliter Array in a Microfluidic Device. *Lab Chip* **2009**, *9* (1), 44–49.
- (42) Clausell-Tormos, J.; Lieber, D.; Baret, J.-C. C.; El-Harrak, A.; Miller, O. J.; Frenz, L.; Blouwolff, J.; Humphry, K. J.; Köster,

- S.; Duan, H.; Holtze, C.; Weitz, D. A.; Griffiths, A. D.; Merten, C. A. Droplet-Based Microfluidic Platforms for the Encapsulation and Screening of Mammalian Cells and Multicellular Organisms. *Chem. Biol.* **2008**, *15* (5), 427–437.
- (43) Lagus, T. P.; Edd, J. F. A Review of the Theory, Methods and Recent Applications of High-Throughput Single-Cell Droplet Microfluidics. *J. Phys. D: Appl. Phys.* **2013**, *46* (114005), 21.
- (44) Edd, J. F.; Di Carlo, D.; Humphry, K. J.; Köster, S.; Irimia, D.; Weitz, D. A.; Toner, M. Controlled Encapsulation of Single-Cells into Monodisperse Picolitre Drops. *Lab Chip* **2008**, *8* (8), 1262–1264.
- (45) Chabert, M.; Viovy, J.-L. Microfluidic High-Throughput Encapsulation and Hydrodynamic Self-Sorting of Single Cells. *Proc. Natl. Acad. Sci.* **2008**, *105* (9), 3191–3196.
- (46) Joensson, H. N.; Andersson Svahn, H. Droplet Microfluidics - A Tool for Single-Cell Analysis. *Angew. Chemie - Int. Ed.* **2012**, *51* (49), 12176–12192.
- (47) Lindström, S.; Andersson-Svahn, H. Miniaturization of Biological Assays - Overview on Microwell Devices for Single-Cell Analyses. *Biochim. Biophys. Acta - Gen. Subj.* **2011**, *1810* (3), 308–316.
- (48) Taylor, L. C.; Walt, D. R. Application of High-Density Optical Microwell Arrays in a Live-Cell Biosensing System. *Anal. Biochem.* **2000**, *278* (2), 132–142.
- (49) Ostuni, E.; Chen, C. S.; Ingber, D. E.; Whitesides, G. M. Selective Deposition of Proteins and Cells in Arrays of Microwells. *Langmuir* **2001**, *17* (9), 2828–2834.
- (50) Rettig, J. R.; Folch, A. Large-Scale Single-Cell Trapping and Imaging Using Microwell Arrays. *Anal. Chem.* **2005**, *77* (17), 5628–5634.
- (51) Love, J. C.; Ronan, J. L.; Grotenbreg, G. M.; Van Der Veen, A. G.; Ploegh, H. L. A Microengraving Method for Rapid Selection of Single Cells Producing Antigen-Specific Antibodies. *Nat. Biotechnol.* **2006**, *24* (6), 703–707.
- (52) Revzin, A.; Sekine, K.; Sin, A.; Tompkins, R. G.; Toner, M. Development of a Microfabricated Cytometry Platform for Characterization and Sorting of Individual Leukocytes. *Lab Chip* **2005**, *5* (1), 30–37.
- (53) Revzin, A.; Tompkins, R. G.; Toner, M. Surface Engineering with Poly(ethylene Glycol) Photolithography to Create High-Density Cell Arrays on Glass. *Langmuir* **2003**, *19* (23), 9855–9862.
- (54) Tokimitsu, Y.; Kishi, H.; Kondo, S.; Honda, R.; Tajiri, K.; Motoki, K.; Ozawa, T.; Kadowaki, S.; Obata, T.; Fujiki, S.; Tateno, C.; Takaishi, H.; Chayama, K.; Yoshizato, K.; Tamiya, E.; Sugiyama, T.; Muraguchi, A. Single Lymphocyte Analysis with a Microwell Array Chip. *Cytom. Part A* **2007**, *71* (12), 1003–1010.
- (55) Kurth, I.; Franke, K.; Pompe, T.; Bornhäuser, M.; Werner, C. Hematopoietic Stem and Progenitor Cells in Adhesive Microcavities. *Integr. Biol.* **2009**, *1* (5–6), 427–434.
- (56) Deutsch, M.; Deutsch, A.; Shirihai, O.; Hurevich, I.; Afrimzon, E.; Shafran, Y.; Zurgil, N. A Novel Miniature Cell Retainer for Correlative High-Content Analysis of Individual Untethered Non-Adherent Cells. *Lab Chip* **2006**, *6* (8), 995–1000.
- (57) Deutsch, A.; Zurgil, N.; Hurevich, I.; Shafran, Y.; Afrimzon, E.; Lebovich, P.; Deutsch, M. Microplate Cell-Retaining Methodology for High-Content Analysis of Individual Non-Adherent Unanchored Cells in a Population. *Biomed. Microdevices* **2006**, *8* (4), 361–374.
- (58) Chin, V. I.; Taupin, P.; Sanga, S.; Scheel, J.; Gage, F. H.; Bhatia, S. N. Microfabricated Platform for Studying Stem Cell Fates. *Biotechnol. Bioeng.* **2004**, *88* (3), 399–415.
- (59) Figueroa, X.; Cooksey, G.; Votaw, S.; Horowitz, L.; Folch, A. Large-Scale Investigation of the Olfactory Receptor Space Using a Microfluidic Microwell Array. *Lab Chip* **2010**, *10* (9), 1120–1127.
- (60) Kumar, P. T.; Vriens, K.; Cornaglia, M.; Gijs, M.; Kokalj, T.; Thevissen, K.; Geeraerd, A.; Cammue, B. P. A.; Puers, R.; Lammertyn, J. Digital Microfluidics for Time-Resolved Cytotoxicity Studies on Single Non-Adherent Yeast Cells. *Lab Chip* **2015**, *15* (8), 1852–1860.
- (61) Witters, D.; Toffalini, F.; Puers, R.; Lammertyn, J. Digital Microfluidic Femtoliter Droplet Printing : A Versatile Tool for Single-Molecule Detection of Nucleic Acids and Proteins. In *17th International Conference on Miniaturized Systems for Chemistry and Life Sciences (MicroTAS 2013)*; 2013; pp 296–298.
- (62) Witters, D.; Knez, K.; Ceysens, F.; Puers, R.; Lammertyn, J. Digital Microfluidics-Enabled Single-Molecule Detection by Printing and Sealing Single Magnetic Beads in Femtoliter Droplets. *Lab Chip* **2013**, *13* (11), 2047–2054.
- (63) Kang, D. K.; Monsur Ali, M.; Zhang, K.; Pone, E. J.; Zhao, W. Droplet Microfluidics for Single-Molecule and Single-Cell Analysis in Cancer Research, Diagnosis and Therapy. *Trends Anal. Chem.* **2014**, *58*, 145–153.
- (64) Gong, Y.; Ogunniyi, A. O.; Love, J. C. Massively Parallel Detection of Gene Expression in Single Cells Using Subnanolitre Wells. *Lab Chip* **2010**, *10* (18), 2334–2337.
- (65) Gole, J.; Gore, A.; Richards, A.; Chiu, Y.-J.; Fung, H.-L.; Bushman, D.; Chiang, H.-I.; Chun, J.; Lo, Y.-H.; Zhang, K. Massively Parallel Polymerase Cloning and Genome Sequencing of Single Cells Using Nanoliter Microwells. *Nat. Biotechnol.* **2013**, *31* (12), 1126–1132.
- (66) Kumaresan, P.; Yang, C. J.; Cronier, S. A.; Blazej, R. G.; Mathies, R. A. High-Throughput Single Copy DNA Amplification and Cell Analysis in Engineered Nanoliter Droplets. *Anal. Chem.* **2008**, *80* (10), 3522–3529.
- (67) Zeng, Y.; Novak, R.; Shuga, J.; Smith, M. T.; Mathies, R. A. High-Performance Single Cell Genetic Analysis Using Microfluidic Emulsion Generator Arrays. *Anal. Chem.* **2010**, *82* (8), 3183–3190.
- (68) Novak, R.; Zeng, Y.; Shuga, J.; Venugopalan, G.; Fletcher, D. A.; Smith, M. T.; Mathies, R. A. Single-Cell Multiplex Gene Detection and Sequencing with Microfluidically Generated Agarose Emulsions. *Angew. Chemie - Int. Ed.* **2011**, *50* (2), 390–395.
- (69) Klein, A. M.; Mazutis, L.; Akartuna, I.; Tallapragada, N.; Veres, A.; Li, V.; Peshkin, L.; Weitz, D. A.; Kirschner, M. W. Droplet Barcoding for Single-Cell Transcriptomics Applied to Embryonic Stem Cells. *Cell* **2015**, *161* (5), 1187–1201.
- (70) Macosko, E. Z.; Basu, A.; Satija, R.; Nemesh, J.; Shekhar, K.; Goldman, M.; Tirosh, I.; Bialas, A. R.; Kamitaki, N.; Martersteck, E. M.; Trombetta, J. J.; Weitz, D. A.; Sanes, J. R.; Shalek, A. K.; Regev, A.; McCarroll, S. A. Highly Parallel Genome-Wide Expression Profiling of Individual Cells Using Nanoliter Droplets. *Cell* **2015**, *161* (5), 1202–1214.
- (71) Leng, X.; Zhang, W.; Wang, C.; Cui, L.; Yang, C. J. Agarose Droplet Microfluidics for Highly Parallel and Efficient Single Molecule Emulsion PCR. *Lab Chip* **2010**, *10*, 2841–2843.
- (72) Zhang, H.; Jenkins, G.; Zou, Y.; Zhu, Z.; Yang, C. J. Massively Parallel Single-Molecule and Single-Cell Emulsion Reverse Transcription Polymerase Chain Reaction Using Agarose Droplet Microfluidics. *Anal. Chem.* **2012**, *84* (8), 3599–3606.
- (73) Zhu, Z.; Zhang, W.; Leng, X.; Zhang, M.; Guan, Z.; Lu, J.; Yang, C. J. Highly Sensitive and Quantitative Detection of Rare Pathogens through Agarose Droplet Microfluidic Emulsion PCR at the Single-Cell Level. *Lab Chip* **2012**, *12* (20), 3907–3913.
- (74) Chao, T.-C.; Ros, A. Microfluidic Single-Cell Analysis of Intracellular Compounds. *J. R. Soc. Interface* **2008**, *5*, S139–S150.
- (75) Rakszewska, A.; Tel, J.; Chokkalingam, V.; Huck, W. T. One Drop at a Time: Toward Droplet Microfluidics as a Versatile Tool for Single-Cell Analysis. *NPG Asia Mater.* **2014**, *6* (10), e133.
- (76) Rival, A.; Jary, D.; Delattre, C.; Fouillet, Y.; Castellan, G.; Bellemin-Comte, A.; Gidrol, X. EWOD-Based Microfluidic Chip for Single-Cell Isolation, mRNA Purification and Subsequent Multiplex qPCR. *Lab Chip* **2014**, *14*, 3739–3749.



- (77) Dimov, I. K.; Lu, R.; Lee, E. P.; Seita, J.; Sahoo, D.; Park, S.; Weissman, I. L.; Lee, L. P. Discriminating Cellular Heterogeneity Using Microwell-Based RNA Cytometry. *Nat. Commun.* **2014**, *5*, 3451.
- (78) Huebner, A.; Srisa-art, M.; Holt, D.; Abell, C.; Hollfelder, F.; DeMello, A. J.; Edel, J. B. Quantitative Detection of Protein Expression in Single Cells Using Droplet Microfluidics. *Chem Commun* **2007**, *2* (12), 1218–1220.
- (79) Huebner, A.; Olguin, L. F.; Bratton, D.; Whyte, G.; Huck, W. T. S.; de Mello, A. J.; Edel, J. B.; Abell, C.; Hollfelder, F. Development of Quantitative Cell-Based Enzyme Assays in Microdroplets. *Anal. Chem.* **2008**, *80* (10), 3890–3896.
- (80) Abbaspourrad, A.; Zhang, H.; Tao, Y.; Cui, N.; Asahara, H.; Zhou, Y.; Yue, D.; Koehler, S. A.; Ung, L. W.; Heyman, J.; Ren, Y.; Ziblat, R.; Chong, S.; Weitz, D. A. Label-Free Single-Cell Protein Quantification Using a Drop-Based Mix-and-Read System. *Sci. Rep.* **2015**, *5*, 12756.
- (81) He, M.; Edgar, J. S.; Jeffries, G. D. M.; Lorenz, R. M.; Shelby, J. P.; Chiu, D. T. Selective Encapsulation of Single Cells and Subcellular Organelles into Picoliter- and Femtoliter-Volume Droplets. *Anal. Chem.* **2005**, *77* (6), 1539–1544.
- (82) Eyer, K.; Stratz, S.; Kuhn, P.; Küster, S. K.; Dittrich, P. S. Implementing Enzyme-Linked Immunosorbent Assays on a Microfluidic Chip to Quantify Intracellular Molecules in Single Cells. *Anal. Chem.* **2013**, *85* (6), 3280–3287.
- (83) Xue, M.; Wei, W.; Su, Y.; Kim, J.; Shin, Y. S.; Mai, W. X.; Nathanson, D. A.; Heath, J. R. Chemical Methods for the Simultaneous Quantitation of Metabolites and Proteins from Single Cells. *J. Am. Chem. Soc.* **2015**, *137* (12), 4066–4069.
- (84) Shi, Q.; Qin, L.; Wei, W.; Geng, F.; Fan, R.; Shin, Y. S.; Guo, D.; Hood, L.; Mischel, P. S.; Heath, J. R. Single-Cell Proteomic Chip for Profiling Intracellular Signaling Pathways in Single Tumor Cells. *Proc. Natl. Acad. Sci. U. S. A.* **2012**, *109* (2), 419–424.
- (85) Ma, C.; Fan, R.; Ahmad, H.; Shi, Q.; Comin-Anduix, B.; Chodon, T.; Koya, R. C.; Liu, C.-C.; Kwong, G. A.; Radu, C. G.; Ribas, A.; Heath, J. R. A Clinical Microchip for Evaluation of Single Immune Cells Reveals High Functional Heterogeneity in Phenotypically Similar T Cells. *Nat. Med.* **2011**, *17* (6), 738–743.
- (86) Park, M. C.; Hur, J. Y.; Kwon, K. W.; Park, S.-H.; Suh, K. Y. Pumpless, Selective Docking of Yeast Cells inside a Microfluidic Channel Induced by Receding Meniscus. *Lab Chip* **2006**, *6* (8), 988–994.
- (87) Kim, J. J.; Sinkala, E.; Herr, A. E. High-Selectivity Cytology via Lab-on-a-Disc Western Blotting of Individual Cells. *Lab Chip* **2017**, *17* (5), 855–863.
- (88) Yamauchi, K. A.; Herr, A. E. Subcellular Western Blotting of Single Cells. *Microsystems Nanoeng.* **2017**, *3* (September 2016), 16079.
- (89) Beneyton, T.; Thomas, S.; Griffiths, A. D.; Nicaud, J.-M.; Drevelle, A.; Rossignol, T. Droplet-Based Microfluidic High-Throughput Screening of Heterologous Enzymes Secreted by the Yeast *Yarrowia Lipolytica*. *Microb. Cell Fact.* **2017**, *16* (1), 18.
- (90) Chokkalingam, V.; Tel, J.; Wimmers, F.; Liu, X.; Semenov, S.; Thiele, J.; Figdor, C. G.; Huck, W. T. S. Probing Cellular Heterogeneity in Cytokine-Secreting Immune Cells Using Droplet-Based Microfluidics. *Lab Chip* **2013**, *13* (24), 4740–4744.
- (91) Konry, T.; Golberg, A.; Yarmush, M. Live Single Cell Functional Phenotyping in Droplet Nano-Liter Reactors. *Sci. Rep.* **2013**, *3*, 3179.
- (92) Mazutis, L.; Gilbert, J.; Ung, W. L.; Weitz, D. A.; Griffiths, A. D.; Heyman, J. A. Single-Cell Analysis and Sorting Using Droplet-Based Microfluidics. *Nat. Protoc.* **2013**, *8* (5), 870–891.
- (93) Debs, B. E.; Utharala, R.; Balyasnikova, I. V.; Griffiths, A. D.; Merten, C. A. Functional Single-Cell Hybridoma Screening Using Droplet-Based Microfluidics. *Proc. Natl. Acad. Sci.* **2012**, *109* (29), 11570–11575.
- (94) Story, C. M.; Papa, E.; Hu, C.-C. A.; Ronan, J. L.; Herlihy, K.; Ploegh, H. L.; Love, J. C. Profiling Antibody Responses by Multiparametric Analysis of Primary B Cells. *Proc. Natl. Acad. Sci.* **2008**, *105* (46), 17902–17907.
- (95) Bradshaw, E. M.; Kent, S. C.; Tripuraneni, V.; Orban, T.; Hidde, L.; Hafler, D. A.; Love, J. C. Concurrent Detection of Secreted Products from Human Lymphocytes by Microengraving: Cytokines and Antigen-Reactive Antibodies. *Clin. Immunol.* **2009**, *129* (1), 10–18.
- (96) Ogunniyi, A.; Story, C.; Papa, E.; Guillen, E.; Love, C. Screening Individual Hybridomas by Microengraving to Discover Monoclonal Antibodies. *Nat. Protoc.* **2009**, *4* (5), 767–782.
- (97) Joensson, H. N.; Samuels, M. L.; Bronzes, E. R.; Medkova, M.; Uhlén, M.; Link, D. R.; Andersson-Svahn, H. Detection and Analysis of Low-Abundance Cell-Surface Biomarkers Using Enzymatic Amplification in Microfluidic Droplets. *Angew. Chemie - Int. Ed.* **2009**, *48* (14), 2518–2521.
- (98) Konry, T.; Smolina, I.; Yarmush, J. M.; Irimia, D.; Yarmush, M. L. Ultrasensitive Detection of Low-Abundance Surface-Marker Protein Using Isothermal Rolling Circle Amplification in a Microfluidic Nanoliter Platform. *Small* **2011**, *7* (3), 395–400.
- (99) Li, L.; Wang, Q.; Feng, J.; Tong, L.; Tang, B. Highly Sensitive and Homogeneous Detection of Membrane Protein on a Single Living Cell by Aptamer and Nicking Enzyme Assisted Signal Amplification Based on Microfluidic Droplets. *Anal. Chem.* **2014**, *86* (10), 5101–5107.
- (100) Park, S.; Lee, J. Y.; Hong, S.; Lee, S. H.; Dimov, I. K.; Lee, H.; Suh, S.; Pan, Q.; Li, K.; Wu, A. M.; Mumenthaler, S. M.; Mallick, P.; Lee, L. P. Dual Transcript and Protein Quantification in a Massive Single Cell Array. *Lab Chip* **2016**, *16* (19), 3682–3688.
- (101) Friedrich, S. M.; Zec, H. C.; Wang, T.-H. Analysis of Single Nucleic Acid Molecules in Micro- and Nano-Fluidics. *Lab Chip* **2016**, *16* (5), 790–811.
- (102) Freire, S. L. S. Perspectives on Digital Microfluidics. *Sensors Actuators A Phys.* **2016**, *250*, 15–28.
- (103) Shembekar, N.; Chaipan, C.; Utharala, R.; Merten, C. A. Droplet-Based Microfluidics in Drug Discovery, Transcriptomics and High-Throughput Molecular Genetics. *Lab Chip* **2016**, *16* (8), 1314–1331.
- (104) Zhang, Y.; Jiang, H. R. A Review on Continuous-Flow Microfluidic PCR in Droplets: Advances, Challenges and Future. *Anal. Chim. Acta* **2016**, *914*, 7–16.
- (105) Dong, L.; Meng, Y.; Sui, Z.; Wang, J.; Wu, L.; Fu, B. Comparison of Four Digital PCR Platforms for Accurate Quantification of DNA Copy Number of a Certified Plasmid DNA Reference Material. *Sci. Rep.* **2015**, *5*, 13174.
- (106) Bio-Rad. QX200™ Droplet Digital™ PCR System. Bio-Rad Laboratories, Inc 2017, pp 1–16.
- (107) RainDance Technologies. RainDrop Plus™ Digital PCR System - Product Brief. RainDance Technologies, Inc: U.S.A. 2016, pp 1–2.
- (108) Huggett, J. F.; Foy, C. A.; Benes, V.; Emslie, K.; Garson, J. A.; Haynes, R.; Hellemans, J.; Kubista, M.; Mueller, R. D.; Nolan, T.; Pfaffl, M. W.; Shipley, G. L.; Vandesompele, J.; Wittwer, C. T.; Bustin, S. A. The Digital MIQE Guidelines: Minimum Information for Publication of Quantitative Digital PCR Experiments. *Clin. Chem.* **2013**, *59* (6), 892–902.
- (109) Kang, D.-K. D.-K.; Ali, M. M.; Zhang, K.; Huang, S. S.; Peterson, E.; Digman, M. A.; Gratton, E.; Zhao, W. Rapid Detection of Single Bacteria in Unprocessed Blood Using Integrated Comprehensive Droplet Digital Detection. *Nat. Commun.* **2014**, *5*, 5427.
- (110) Wang, P.; Jing, F.; Li, G.; Wu, Z.; Cheng, Z.; Zhang, J.; Zhang, H.; Jia, C.; Jin, Q.; Mao, H.; Zhao, J. Absolute Quantification of Lung Cancer Related microRNA by Droplet Digital PCR. *Biosens. Bioelectron.* **2015**, *74*, 836–842.
- (111) Qin, Z.; Ljubimov, V. A.; Zhou, C.; Tong, Y.; Liang, J. Cell-

- Free Circulating Tumor DNA in Cancer. *Chin. J. Cancer* **2016**, *35*, 36.
- (112) Madic, J.; Zocevic, A.; Senlis, V.; Fradet, E.; Andre, B.; Muller, S.; Dangla, R.; Droniou, M. E. Three-Color Crystal Digital PCR. *Biomol. Detect. Quantif.* **2016**, *10*, 34–46.
- (113) STILLA. Naica System for Crystal Digital PCR. STILLA Technologies: France 2017, pp 1–4.
- (114) Norian, H.; Field, R. M.; Kymissis, I.; Shepard, K. L. An Integrated CMOS Quantitative-Polymerase-Chain-Reaction Lab-on-Chip for Point-of-Care Diagnostics. *Lab Chip* **2014**, *14* (20), 4076–4084.
- (115) Shuga, J.; Zeng, Y.; Novak, R.; Lan, Q.; Tang, X.; Rothman, N.; Vermeulen, R.; Li, L.; Hubbard, A.; Zhang, L.; Mathies, R. A.; Smith, M. T. Single Molecule Quantitation and Sequencing of Rare Translocations Using Microfluidic Nested Digital PCR. *Nucleic Acids Res.* **2013**, *41* (16), e159.
- (116) Vogelstein, B.; Kinzler, K. W. Digital PCR. *Proc. Natl. Acad. Sci. U. S. A.* **1999**, *96* (16), 9236–9241.
- (117) Formulatrix. Constellation User's Guide. 2014, p 10.
- (118) Ding, X.; Mu, Y. Digital Nucleic Acid Detection Based on Microfluidic Lab-on-a-Chip Devices. In *Lab-on-a-Chip Fabrication and Application*; InTech, 2016.
- (119) Blow, N. PCR's next Frontier. *Nat. Methods* **2007**, *4* (10), 869–875.
- (120) Ottesen, E. A.; Hong, J. W.; Quake, S. R.; Leadbetter, J. R. Microfluidic Digital PCR Enables Multigene Analysis of Individual Environmental Bacteria. *Science* **2006**, *314* (5804), 1464–1467.
- (121) Ramakrishnan, R.; Qin, J.; Jones, R. C.; Suzanne Weaver, L. Integrated Fluidic Circuits (IFCs) for Digital PCR. *Methods Mol. Biol.* **2013**, *949*, 423–431.
- (122) Fluidigm. The BioMark 96.96 Dynamic Array - Product News. Fluidigm Corporation: USA 2017, pp 1–2.
- (123) Oehler, V. G.; Qin, J.; Ramakrishnan, R.; Facer, G.; Ananthnarayan, S.; Cummings, C.; Deininger, M.; Shah, N.; McCormick, F.; Willis, S.; Daridon, A.; Unger, M.; Radich, J. P. Absolute Quantitative Detection of ABL Tyrosine Kinase Domain Point Mutations in Chronic Myeloid Leukemia Using a Novel Nanofluidic Platform and Mutation-Specific PCR. *Leukemia* **2009**, *23* (2), 396–399.
- (124) Fan, H. C.; Blumenfeld, Y. J.; El-Sayed, Y. Y.; Chueh, J.; Quake, S. R. Microfluidic Digital PCR Enables Rapid Prenatal Diagnosis of Fetal Aneuploidy. *Am. J. Obstet. Gynecol.* **2009**, *200* (5), 543.e1–543.e7.
- (125) Life Technologies. QuantStudio™ 3D Digital PCR System - Product Bulletin. Thermo Fisher Scientific, Inc 2014, pp 1–8.
- (126) Conte, D.; Verri, C.; Borzi, C.; Suatoni, P.; Pastorino, U.; Sozzi, G.; Fortunato, O. Novel Method to Detect microRNAs Using Chip-Based QuantStudio 3D Digital PCR. *BMC Genomics* **2015**, *16* (1), 849.
- (127) Klančnik, A.; Toplak, N.; Kovač, M.; Marquis, H.; Jeršek, B. Quantification of *Listeria monocytogenes* Cells with Digital PCR and Their Biofilm Cells with Real-Time PCR. *J. Microbiol. Methods* **2015**, *118*, 37–41.
- (128) Kaitu'u-Lino, T. J.; Hastie, R.; Cannon, P.; Lee, S.; Stock, O.; Hannan, N. J.; Hiscock, R.; Tong, S. Stability of Absolute Copy Number of Housekeeping Genes in Preeclamptic and Normal Placentas, as Measured by Digital PCR. *Placenta* **2014**, *35* (12), 1106–1109.
- (129) Kinz, E.; Leisher, A.; Lang, A. H.; Drexel, H.; Muendlein, A. Accurate Quantitation of JAK2 V617F Allele Burden by Array-Based Digital PCR. *Int. J. Lab. Hematol.* **2015**, *37* (2), 217–224.
- (130) Tröger, V.; Niemann, K.; Gärtig, C.; Kuhlmeier, D. Isothermal Amplification and Quantification of Nucleic Acids and Its Use in Microsystems. *Nanomedicine Nanotechnol.* **2015**, *6* (3), 282.
- (131) Zanolli, L. M.; Spoto, G. Isothermal Amplification Methods for the Detection of Nucleic Acids in Microfluidic Devices. *Biosensors* **2013**, *3* (1), 18–43.
- (132) Rane, T. D.; Chen, L.; Zec, H. C.; Wang, T.-H. Microfluidic Continuous Digital Loop-Mediated Isothermal Amplification (LAMP). *Lab Chip* **2015**, *15* (3), 776–782.
- (133) Schuler, F.; Schwemmer, F.; Trotter, M.; Wadle, S.; Zengerle, R.; von Stetten, F.; Paust, N. Centrifugal Step Emulsification Applied for Absolute Quantification of Nucleic Acids by Digital Droplet RPA. *Lab Chip* **2015**, *15* (13), 2759–2766.
- (134) Piepenburg, O.; Williams, C. H.; Stemple, D. L.; Armes, N. A. DNA Detection Using Recombination Proteins. *PLoS Biol.* **2006**, *4* (7), 1115–1121.
- (135) Gansen, A.; Herrick, A. M.; Dimov, I. K.; Lee, L. P.; Chiu, D. T. Digital LAMP in a Sample Self-Digitization (SD) Chip. *Lab Chip* **2012**, *12* (12), 2247–2254.
- (136) Zhu, Q.; Gao, Y.; Yu, B.; Ren, H.; Qiu, L.; Han, S.; Jin, W.; Jin, Q.; Mu, Y. Self-Priming Compartmentalization Digital LAMP for Point-of-Care. *Lab Chip* **2012**, *12* (22), 4755–4763.
- (137) Shen, F.; Davydova, E. K.; Du, W.; Kreutz, J. E.; Piepenburg, O.; Ismagilov, R. F. Digital Isothermal Quantification of Nucleic Acids via Simultaneous Chemical Initiation of Recombinase Polymerase Amplification Reactions on SlipChip. *Anal. Chem.* **2011**, *83* (9), 3533–3540.
- (138) Rodriguez-Manzano, J.; Karymov, M. A.; Begolo, S.; Selck, D. A.; Zhukov, D. V.; Jue, E.; Ismagilov, R. F. Reading Out Single-Molecule Digital RNA and DNA Isothermal Amplification in Nanoliter Volumes with Unmodified Camera Phones. *ACS Nano* **2016**, *10* (3), 3102–3113.
- (139) Blainey, P. C.; Quake, S. R. Digital MDA for Enumeration of Total Nucleic Acid Contamination. *Nucleic Acids Res.* **2011**, *39* (4), e19.
- (140) Guan, W.; Chen, L.; Rane, T. D.; Wang, T.-H. Droplet Digital Enzyme-Linked Oligonucleotide Hybridization Assay for Absolute RNA Quantification. *Sci. Rep.* **2015**, *5*, 13795.
- (141) Bustin, S. a.; Benes, V.; Garson, J. a.; Hellemans, J.; Huggett, J.; Kubista, M.; Mueller, R.; Nolan, T.; Pfaffl, M. W.; Shipley, G. L.; Vandesompele, J.; Wittwer, C. T. The MIQE guidelines: Minimum Information for Publication of Quantitative Real-Time PCR Experiments. *Clin. Chem.* **2009**, *55* (4), 611–622.
- (142) Schaerli, Y.; Wootton, R. C.; Robinson, T.; Stein, V.; Dunsby, C.; Neil, M. A. A.; French, P. M. W.; deMello, A. J.; Abell, C.; Hollfelder, F. Continuous-Flow Polymerase Chain Reaction of Single-Copy DNA in Microfluidic Microdroplets. *Anal. Chem.* **2009**, *81* (1), 302–306.
- (143) Taly, V.; Kelly, B. T.; Griffiths, A. D. Droplets as Microreactors for High-Throughput Biology. *ChemBioChem* **2007**, *8* (3), 263–272.
- (144) Bartlett, J. M. S.; Stirling, D. A Short History of the Polymerase Chain Reaction. In *PCR Protocols*; Humana Press: New Jersey, 2003; pp 3–6.
- (145) Sanders, R.; Mason, D. J.; Foy, C. A.; Huggett, J. F. Evaluation of Digital PCR for Absolute RNA Quantification. *PLoS One* **2013**, *8* (9), e75296.
- (146) Borst, A.; Box, A. T. A.; Fluit, A. C. False-Positive Results and Contamination in Nucleic Acid Amplification Assays: Suggestions for a Prevent and Destroy Strategy. *Eur. J. Clin. Microbiol. Infect. Dis.* **2004**, *23* (4), 289–299.
- (147) Song, L.; Shan, D.; Zhao, M.; Pink, B. A.; Minnehan, K. A.; York, L.; Gardel, M.; Sullivan, S.; Phillips, A. F.; Hayman, R. B.; Walt, D. R.; Duffy, D. C. Direct Detection of Bacterial Genomic DNA at Sub-Femtomolar Concentrations Using Single Molecule Arrays. *Anal. Chem.* **2013**, *85* (3), 1932–1939.
- (148) Rothberg, J. M.; Leamon, J. H. The Development and Impact of 454 Sequencing. *Nat. Biotechnol.* **2008**, *26* (10), 1117–1124.
- (149) Reuter, J. A.; Spacek, D. V.; Snyder, M. P. High-Throughput Sequencing Technologies. *Mol. Cell* **2015**, *58* (4), 586–597.
- (150) Rothberg, J. M.; Hinz, W.; Rearick, T. M.; Schultz, J.; Mileski, W.; Davey, M.; Leamon, J. H.; Johnson, K.; Milgrew, M. J.; Edwards, M.; Hoon, J.; Simons, J. F.; Marran, D.; Myers, J. W.; Davidson, J. F.; Branting, A.; Nobile, J. R.; Puc, B. P.; Light, D.; Clark, T. a.; Huber, M.; Branciforte, J. T.; Stoner, I. B.; Cawley, S. E.; Lyons, M.; Fu, Y.; Homer, N.; Sedova, M.; Miao, X.; Reed, B.; Sabina, J.; Feierstein, E.; Schorn, M.; Alanjary,

- M.; Dimalanta, E.; Dressman, D.; Kasinskas, R.; Sokolsky, T.; Fidanza, J. a; Namsaraev, E.; McKernan, K. J.; Williams, A.; Roth, G. T.; Bustillo, J. An Integrated Semiconductor Device Enabling Non-Optical Genome Sequencing. *Nature* **2011**, *475* (7356), 348–352.
- (151) Eid, J. J.; Fehr, A.; Gray, J.; Luong, K.; Lyle, J.; Otto, G.; Peluso, P.; Rank, D. D.; Baybayan, P.; Bettman, B.; Bibillo, A.; Bjornson, K.; Chaudhuri, B.; Christians, F.; Cicero, R.; Clark, S.; Dalal, R.; DeWinter, A.; Dixon, J.; Foquet, M.; Gaertner, A.; Hardenbol, P.; Heiner, C.; Hester, K.; Holden, D.; Kearns, G.; Kong, X.; Kuse, R.; Lacroix, Y.; Lin, S.; Lundquist, P.; Ma, C.; Marks, P.; Maxham, M.; Murphy, D.; Park, I.; Pham, T.; Phillips, M.; Roy, J.; Sebra, R.; Shen, G.; Sorenson, J.; Tomaney, A.; Travers, K. K. K.; Trulson, M.; Vieceli, J.; Wegener, J.; Wu, D.; Yang, A.; Zaccarin, D.; Zhao, P.; Zhong, F.; Korch, J.; Turner, S. S. Real-Time DNA Sequencing from Single Polymerase Molecules. *Science* **2009**, *323* (5910), 133–138.
- (152) Levene, M. J.; Korch, J.; Turner, S. W.; Foquet, M.; Craighead, H. G.; Webb, W. W. Zero-Mode Waveguides for Single-Molecule Analysis at High Concentrations. *Science* **2003**, *299* (5607), 682–686.
- (153) Rao, A. N.; Grainger, D. W. Biophysical Properties of Nucleic Acids at Surfaces Relevant to Microarray Performance. *Biomater. Sci.* **2014**, *2* (4), 436–436.
- (154) Reisner, W.; Pedersen, J. N.; Austin, R. H. DNA Confinement in Nanochannels: Physics and Biological Applications. *Reports Prog. Phys.* **2012**, *75*, 106601.
- (155) Michaeli, Y.; Ebenstein, Y. Channeling DNA for Optical Mapping. *Nat. Biotechnol.* **2012**, *30* (8), 762–763.
- (156) Kim, Y.; Kim, K. S.; Kounovsky, K. L.; Chang, R.; Jung, G. Y.; DePablo, J. J.; Jo, K.; Schwartz, D. C. Nanochannel Confinement: DNA Stretch Approaching Full Contour Length. *Lab Chip* **2011**, *11* (10), 1721–1729.
- (157) Reccius, C. H.; Mannion, J. T.; Cross, J. D.; Craighead, H. G. Compression and Free Expansion of Single DNA Molecules in Nanochannels. *Phys. Rev. Lett.* **2005**, *95* (26), 268101.
- (158) Lam, E. T.; Hastie, A.; Lin, C.; Ehrlich, D.; Das, S. K.; Austin, M. D.; Deshpande, P.; Cao, H.; Nagarajan, N.; Xiao, M.; Kwok, P.-Y. Genome Mapping on Nanochannel Arrays for Structural Variation Analysis and Sequence Assembly. *Nat. Biotechnol.* **2012**, *30* (8), 771–776.
- (159) Bionanogenomics. NanoChannel Arrays.
- (160) Castillo-Fernandez, O.; Salieb-Beugelaar, G. B.; van Nieuwkastele, J. W.; Bomer, J. G.; Arundell, M.; Samitier, J.; van den Berg, A.; Eijkel, J. C. T. T. Electrokinetic DNA Transport in 20nm-High Nanoslits: Evidence for Movement through a Wall-Adsorbed Polymer Nanogel. *Electrophoresis* **2011**, *32* (18), 2402–2409.
- (161) Balducci, A. G.; Tang, J.; Doyle, P. S. Electrophoretic Stretching of DNA Molecules in Cross-Slot Nanoslit Channels. *Macromolecules* **2008**, *41*, 9914–9918.
- (162) Jo, K.; Dhir, D. M.; Odijk, T.; de Pablo, J. J.; Graham, M. D.; Runnheim, R.; Forrest, D.; Schwartz, D. C. A Single-Molecule Barcoding System Using Nanoslits for DNA Analysis. *Proc. Natl. Acad. Sci. U. S. A.* **2007**, *104* (8), 2673–2678.
- (163) Reisner, W.; Larsen, N. B.; Flyvbjerg, H.; Tegenfeldt, J. O.; Kristensen, A. Directed Self-Organization of Single DNA Molecules in a Nanoslit via Embedded Nanopit Arrays. *Proc. Natl. Acad. Sci. U. S. A.* **2009**, *106* (1), 79–84.
- (164) Xu, W.; Muller, S. J. Polymer-Monovalent Salt-Induced DNA Compaction Studied via Single-Molecule Microfluidic Trapping. *Lab Chip* **2012**, *12* (3), 647–651.
- (165) Dylla-Spears, R.; Townsend, J. E.; Jen-Jacobson, L.; Sohn, L. L.; Muller, S. J. Single-Molecule Sequence Detection via Microfluidic Planar Extensional Flow at a Stagnation Point. *Lab Chip* **2010**, *10* (12), 1543–1549.
- (166) Rotman, B. Measurement of Activity of Single Molecules of Beta-D-Galactosidase. *Proc. Natl. Acad. Sci. U. S. A.* **1961**, *47*, 1981–1991.
- (167) Arayanarakool, R.; Shui, L.; Kengen, S. W. M.; Berg van den, A.; Eijkel, J. C. T. Single-Molecule Enzymatic Analysis in a Droplet-Based Microfluidic System. In *16th International Conference on Miniaturized Systems for Chemistry and Life Sciences (MicroTAS 2012)*; 2012; pp 1492–1494.
- (168) Guan, Z.; Zou, Y.; Zhang, M.; Lv, J.; Shen, H.; Yang, P.; Zhang, H.; Zhu, Z.; Yang, C. J. A Highly Parallel Microfluidic Droplet Method Enabling Single-Molecule Counting for Digital Enzyme Detection. *Biomicrofluidics* **2014**, *8* (1), 14110.
- (169) Shim, J. U.; Ranasinghe, R. T.; Smith, C. A.; Ibrahim, S. M.; Hollfelder, F.; Huck, W. T. S.; Klenerman, D.; Abell, C. Ultrarapid Generation of Femtoliter Microfluidic Droplets for Single-Molecule-Counting Immunoassays. *ACS Nano* **2013**, *7* (7), 5955–5964.
- (170) Zhang, H.; Nie, S.; Etsen, C. M.; Wang, R. M.; Walt, D. R. Oil-Sealed Femtoliter Fiber-Optic Arrays for Single Molecule Analysis. *Lab Chip* **2012**, *12* (12), 2229–2239.
- (171) Jung, S. Y.; Liu, Y.; Collier, C. P. Fast Mixing and Reaction Initiation Control of Single-Enzyme Kinetics in Confined Volumes. *Langmuir* **2008**, *24* (9), 4439–4442.
- (172) Ota, S.; Kitagawa, H.; Takeuchi, S. Generation of Femtoliter Reactor Arrays within a Microfluidic Channel for Biochemical Analysis. *Anal. Chem.* **2012**, *84* (15), 6346–6350.
- (173) Sakakihara, S.; Araki, S.; Iino, R.; Noji, H. A Single-Molecule Enzymatic Assay in a Directly Accessible Femtoliter Droplet Array. *Lab Chip* **2010**, *10* (24), 3355–3362.
- (174) Kim, S. H.; Iwai, S.; Araki, S.; Sakakihara, S.; Iino, R.; Noji, H. Large-Scale Femtoliter Droplet Array for Digital Counting of Single Biomolecules. *Lab Chip* **2012**, *12* (23), 4986–4991.
- (175) Rissin, D. M.; Kan, C. W.; Campbell, T. G.; Howes, S. C.; Fournier, D. R.; Song, L.; Piech, T.; Patel, P. P.; Chang, L.; Rivnak, A. J.; Ferrell, E. P.; Randall, J. D.; Provuncher, G. K.; Walt, D. R.; Duffy, D. C. Single-Molecule Enzyme-Linked Immunosorbent Assay Detects Serum Proteins at Subfemtomolar Concentrations. *Nat. Biotechnol.* **2010**, *28* (6), 595–599.
- (176) Kan, C. W.; Rivnak, A. J.; Campbell, T. G.; Piech, T.; Rissin, D. M.; Mösl, M.; Peterca, A.; Niederberger, H.-P.; Minnehan, K. a.; Patel, P. P.; Ferrell, E. P.; Meyer, R. E.; Chang, L.; Wilson, D. H.; Fournier, D. R.; Duffy, D. C. Isolation and Detection of Single Molecules on Paramagnetic Beads Using Sequential Fluid Flows in Microfabricated Polymer Array Assemblies. *Lab Chip* **2012**, *12* (5), 977–985.
- (177) Leirs, K.; Tewari Kumar, P.; Decrop, D.; Pérez-Ruiz, E.; Leblebici, P.; Van Kelst, B.; Compennolle, G.; Meeuws, H.; Van Wesenbeeck, L.; Lagatie, O.; Stuyver, L.; Gils, A.; Lammertyn, J.; Spasic, D. Bioassay Development for Ultrasensitive Detection of Influenza A Nucleoprotein Using Digital ELISA. *Anal. Chem.* **2016**, *88* (17), 8450–8458.
- (178) Pérez-Ruiz, E.; Decrop, D.; Ven, K.; Tripodi, L.; Leirs, K.; Rosseels, J.; van de Wouwer, M.; Geukens, N.; Winderickx, J.; Spasic, D.; Lammertyn, J. Unlocking Tau as Alzheimer's Disease Biomarker: Digital ELISA for the Quantification of Attomolar Tau Concentrations in Blood Plasma. *Anal. Chim. Acta* **2017**, in revision.
- (179) Rissin, D. M.; Fournier, D. R.; Piech, T.; Kan, C. W.; Campbell, T. G.; Song, L.; Chang, L.; Rivnak, A. J.; Patel, P. P.; Provuncher, G. K.; Ferrell, E. P.; Howes, S. C.; Pink, B. A.; Minnehan, K. A.; Wilson, D. H.; Duffy, D. C. Simultaneous Detection of Single Molecules and Singulated Ensembles of Molecules Enables Immunoassays with Broad Dynamic Range. *Anal. Chem.* **2011**, *83* (6), 2279–2285.
- (180) Piraino, F.; Volpetti, F.; Watson, C.; Maerkl, S. J. A Digital-Analog Microfluidic Platform for Patient-Centric Multiplexed Biomarker Diagnostics of Ultralow Volume Samples. *ACS Nano* **2016**, *10*, 1699–1710.
- (181) Ge, S.; Liu, W.; Schlappi, T.; Ismagilov, R. F. Digital, Ultrasensitive, End-Point Protein Measurements with Large Dynamic Range via Brownian Trapping with Drift. *J. Am. Chem. Soc.* **2014**, *136* (42), 14662–14665.

